

TECHNICAL MEMORANDUM

X-246

TRANSONIC AERODYNAMIC CHARACTERISTICS OF A MODEL
OF A PROPOSED SIX-ENGINE HULL-TYPE SEAPLANE
DESIGNED FOR SUPERSONIC FLIGHT

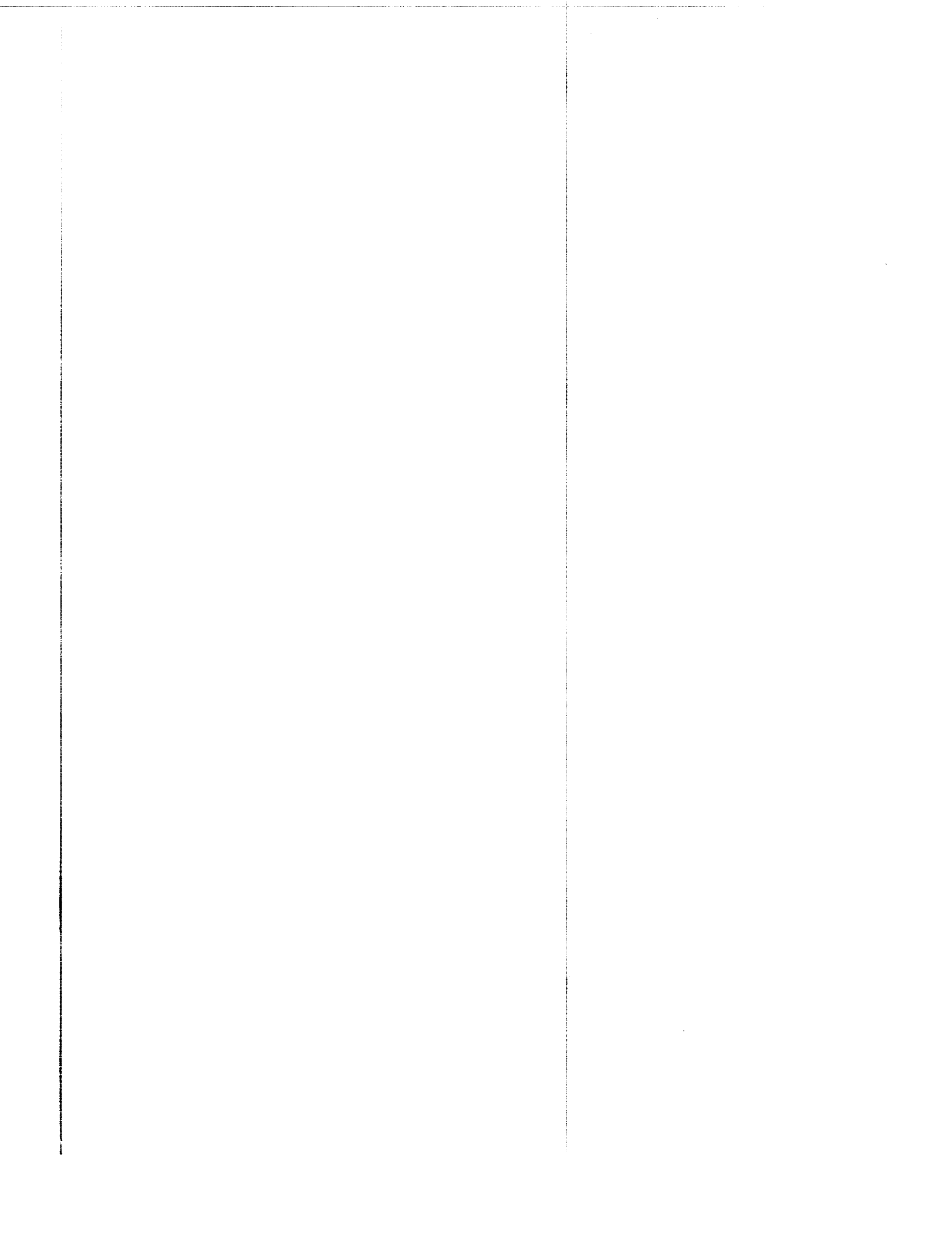
By Dewey E. Wornom

Langley Research Center
Langley Field, Va.

Declassified March 15, 1961

NATIONAL AERONAUTICS AND SPACE ADMINISTRATION
WASHINGTON

March 1960



NATIONAL AERONAUTICS AND SPACE ADMINISTRATION

TECHNICAL MEMORANDUM X-246

TRANSONIC AERODYNAMIC CHARACTERISTICS OF A MODEL
OF A PROPOSED SIX-ENGINE HULL-TYPE SEAPLANE
DESIGNED FOR SUPERSONIC FLIGHT

By Dewey E. Wornom

SUMMARY

Force tests of a model of a proposed six-engine hull-type seaplane were performed in the Langley 8-foot transonic pressure tunnel. The results of these tests have indicated that the model had a subsonic zero-lift drag coefficient of 0.0240 with the highest zero-lift drag coefficient slightly greater than twice the subsonic drag level. Pitchup tendencies were noted for subsonic Mach numbers at relatively high lift coefficients. Wing leading-edge droop increased the maximum lift-drag ratio approximately 8 percent at a Mach number of 0.80 but this effect was negligible at a Mach number of 0.90 and above. The configuration exhibited stable lateral characteristics over the test Mach number range.

INTRODUCTION

The present investigation is part of a general research program to evaluate the aerodynamic and hydrodynamic characteristics of water-based bomber configurations capable of flight at transonic and supersonic speeds. Configurations of previous investigations (refs. 1, 2, and 3) had four engines with various arrangements of engine nacelles or internal ducting or both, which provided a variety of design possibilities. These configurations are characterized by high fineness ratio and small frontal area and are designed in accordance with the area-rule concepts of references 4 to 6. The configuration of the present investigation had six engines and was designed for a sustained cruise Mach number of 1.8 at altitude. Four of the engines were mounted in individual nacelles on the upper surface of the wing; these nacelles were staggered to provide a smooth longitudinal area distribution. The two remaining engines were placed side by side on top of the aft

section of the hull with their inlets located on top of the wing. This configuration was designed in cooperation with the Bureau of Aeronautics, Department of the Navy, and the aircraft industry.

The hydrodynamic investigation to determine the smooth-water resistance, spray characteristics, and the longitudinal stability during take-offs and landings is presented in reference 7. Also included is a brief investigation of rough-water spray characteristics.

In the present investigation, the static longitudinal and lateral aerodynamic characteristics of the six-engine configuration were obtained over a Mach number range from 0.80 to 1.20. The Reynolds number for the tests varied from approximately 1.65×10^6 to 1.8×10^6 based on the wing mean aerodynamic chord.

SYMBOLS

The stability system of axes is used for the presentation of the data.

b	wing span, in.
C_D	drag coefficient, $\frac{\text{Drag}}{qS}$
$C_{D,i}$	total internal-drag coefficient of all engine nacelles based on wing area
$C_{D,o}$	zero-lift drag coefficient
C_L	lift coefficient, $\frac{\text{Lift}}{qS}$
C_{L_α}	lift-curve slope per degree, averaged from $C_L = 0$ to 0.3
C_l	rolling-moment coefficient, $\frac{\text{Rolling moment}}{qSb}$
C_{l_β}	rate of change of rolling-moment coefficient with sideslip angle, $\frac{\partial C_l}{\partial \beta}$
C_m	pitching-moment coefficient, $\frac{\text{Pitching moment about } 0.25\bar{c}}{qS\bar{c}}$

$C_m C_L$	pitching-moment-curve slope, $\frac{\partial C_m}{\partial C_L}$
C_n	yawing-moment coefficient, $\frac{\text{Yawing moment}}{q S_b}$
C_{n_β}	rate of change of yawing-moment coefficient with sideslip angle, $\frac{\partial C_n}{\partial \beta}$
C_Y	side-force coefficient, $\frac{\text{Side force}}{q S}$
C_{Y_β}	rate of change of side-force coefficient with sideslip angle, $\frac{\partial C_Y}{\partial \beta}$
c	local wing chord, in.
\bar{c}	wing mean aerodynamic chord, in.
i_t	angle of incidence of horizontal stabilizer referred to hull base line, positive when trailing edge is down, deg
$(L/D)_{\max}$	maximum lift-drag ratio
M	free-stream Mach number
q	free-stream dynamic pressure, lb/sq ft
S	wing area, sq ft
α	wing chord plane angle of attack, deg
β	angle of sideslip, deg

DESCRIPTION OF CONFIGURATION

The general arrangement of the six-engine hull-type seaplane is shown in figure 1. Pertinent characteristics and dimensions of the full-size seaplane are given in table I.

General Characteristics of Full-Scale Seaplane

The six-engine configuration was designed with a wing area of 1,835 square feet and a gross weight of 220,000 pounds. Six Orenda Iroquois PS-15 turbojet engines, producing a maximum static thrust of 120,000 pounds without afterburners, were used.

Engine location.- Four engines were located in individual nacelles on top of the wing. These nacelles were staggered with the two inboard nacelles forward of the wing and the two outboard nacelles directly over the wing. The two remaining engines, which were located side by side in the after section of the hull, had their inlets located on top of the wing near the 50-percent-chord line.

Wing.- The wing had an aspect ratio of 3.0, a taper ratio of 0.333, and 0° sweepback of the 80-percent-chord line. A 3.5-percent-thick biconvex airfoil section, with the maximum thickness located at the 50-percent-chord line, was used. The wing incidence was 3° with no dihedral or twist.

Hull.- The planing bottom, with a concave-convex-shaped forebody, extended over approximately 96 percent of the fuselage length. The total length-beam ratio of the hull was 13.95 with a maximum beam of 9.2 feet.

Tail group.- The horizontal tail was mounted on top of the vertical tail. This high position was considered necessary for clearance of spray generated by the heavily loaded hull.

Area Curves

The cross-sectional-area curves for the design Mach number of 1.8 and also for a Mach number of 1.0 are presented in figure 2. The area distribution for the tail group was not available and therefore is not included in figure 2; the contribution of the tails to the total area curves would be relatively small. The jet mass flow subtracted from the engine nacelles is represented by an equivalent free-stream tube area of 80 percent of the inlet area.

Model

A 0.02-scale model of the proposed six-engine hull-type seaplane was used for this investigation. Photographs of the sting-mounted model in the Langley 8-foot transonic pressure tunnel are presented in figure 3.

The model wings, tail, hull center, and hull aft sections were constructed of steel; the model hull nose section and wing nacelles were made of Laminac plastic.

Wing leading-edge droop was obtained by tilting a section of the leading edge of each wing semispan down 8°. The drooped sections extended from 0.5lb/2 to 0.94b/2 and were hinged about the 15-percent-chord line.

APPARATUS AND PROCEDURES

Tunnel

The investigation was conducted in the Langley 8-foot transonic pressure tunnel which is a single-return tunnel with a rectangular slotted test section permitting continuous operation through the transonic speed range. Stagnation temperature and dewpoint controls precluded the formation of condensation shocks.

Measurements and Accuracies

Force and moment measurements were obtained by a six-component electrical strain-gage balance internally mounted within the model. Moments are referred to the assumed center of gravity (25 percent of the wing mean aerodynamic chord). All coefficients were based on the wing area of 0.734 square feet and mean aerodynamic chord of 6.438 inches. On the basis of the static calibrations of the electrical strain-gage balance and repeatability of data, the estimated accuracy of the coefficients for a Mach number of 0.80 is within the following limits:

C_L	± 0.02	C_l	± 0.001
C_D	± 0.0015	C_n	± 0.001
C_m	± 0.006	C_y	± 0.005

Since the accuracy is inversely proportional to the dynamic pressure, these values decrease with Mach number. The angle of attack and angle of sideslip were determined within $\pm 0.1^\circ$.

Internal-drag measurements were obtained by pressure survey rakes, consisting of total- and static-pressure tubes, located at the exit of the engine nacelles. Base-pressure measurements were obtained from static-pressure tubes located at the base of the hull.

Tests

Static longitudinal tests of various model configurations were conducted at Mach numbers from 0.80 to 1.20 over an angle-of-attack range from approximately -4° to 17° . The configurations tested included the wing and fuselage alone and in combination with the nacelles and with both nacelles and tail; in addition, wing droop was incorporated for some tests. Most of the tests of the complete model were made with a tail incidence $i_t = 2^{\circ}$ but a few were included with $i_t = -1^{\circ}$. An alternate four-engine configuration was also used for a few longitudinal tests. This configuration was obtained by removing the two outboard wing nacelles of the six-engine configuration and shifting the remaining two inboard wing nacelles outboard and slightly forward. The shifted nacelles were so located that the base of each nacelle still ended at the wing trailing edge and the spanwise location was the same as that of the six-engine outboard nacelles.

Static lateral tests of the various model configurations, excluding wing droop and tail-incidence effects, were conducted over the same Mach number range with an angle-of-sideslip range from approximately -4° to 12° for an angle of attack of approximately 5.7° .

The stagnation pressure for all tests was maintained at 2,120 pounds per square foot. The Reynolds number based on the wing mean aerodynamic chord varied from approximately 1.65×10^6 to 1.80×10^6 .

Corrections

Boundary interference at subsonic velocities has been minimized by the slotted test section and no corrections of the type have been applied. At Mach numbers greater than 1.03 and less than 1.20, boundary reflected disturbances were present and data in this range were not taken. No corrections have been applied for sting-interference effects. The drag data have been adjusted to a condition of free-stream static pressure acting on the model base. The internal-drag coefficients presented in figure 4 have been removed from the drag coefficients presented in this paper.

RESULTS AND DISCUSSION

Longitudinal Characteristics

Lift.—The variation of lift coefficient with angle of attack for the complete six-engine configuration, as shown in the basic longitudinal

data presented in figures 5 to 7, exhibited nonlinearity around $C_L = 0$ ($\alpha \approx 1^\circ$). This nonlinearity of C_L with α is probably due to the flow phenomenon which occurred in the vicinity of the sharp leading edge of the wing at subsonic Mach numbers. (See ref. 8.) The addition of wing leading-edge droop tended to eliminate this nonlinearity. (See fig. 7.)

The variation of lift-curve slope $C_{L\alpha}$ over the test Mach number range for the six-engine configuration is presented in figure 8. This variation follows the usual trend through the transonic speed range.

Drag.- The variation of zero-lift drag coefficient with Mach number for the complete six-engine configuration is presented in figure 9. A value of 0.0240 for zero-lift drag coefficient was measured at subsonic Mach numbers. The highest zero-lift drag coefficient, measured at supersonic speeds, was slightly greater than twice the value noted at subsonic speeds.

The variation of maximum lift-drag ratio with Mach number for the six-engine configuration with and without wing leading-edge droop is presented in figure 10. The six-engine configuration without wing leading-edge droop had a maximum lift-drag ratio of approximately 7.5 at subsonic speeds and followed the usual trend of decreasing with Mach number. The addition of wing leading-edge droop increased the maximum lift-drag ratio approximately 8 percent at a Mach number of 0.80; however, this beneficial effect was negligible at a Mach number of 0.90 and above.

Pitching moment.- The complete six-engine configuration experienced pitchup tendencies (fig. 7) at lift coefficients above 0.7 up to a Mach number of 0.93. The wing leading-edge droop slightly increased the lift coefficient at which pitchup occurred.

The pitching-moment-curve slope C_{mC_L} for the complete six-engine configuration is presented in figure 11. The slopes were determined near a trim-lift coefficient of approximately 0.3. The rearward movement of the aerodynamic center is noted to be approximately 15 percent of the wing mean aerodynamic chord for the test Mach number range.

Alternate four-engine configuration.- Results of tests of the alternate four-engine configuration are presented in figures 12 and 13. The basic longitudinal data of figure 12 show the same nonlinear variation of lift coefficient with angle of attack near zero lift that was noted for the six-engine configuration (figs. 5 to 7). The variation of pitching-moment coefficient over the test lift-coefficient range revealed no pitchup tendencies for the alternate four-engine configuration. The variation of the longitudinal aerodynamic characteristics with Mach number, presented in figure 13, show the usual trends through the transonic speed range.

Lateral Characteristics

The lateral stability characteristics of the six-engine configuration over the test Mach number range at $\alpha \approx 5.7^\circ$ are presented in figure 14. The lateral stability derivatives are presented in figure 15.

In general, the complete six-engine configuration exhibited stable characteristics over the test Mach number range. However, the addition of the wing nacelles had a slight unstable contribution to the configuration.

CONCLUDING REMARKS

The transonic aerodynamic characteristics of a six-engine hull-type seaplane configuration designed for supersonic flight have been investigated. The results of the tests show that:

1. The configuration had a subsonic zero-lift drag coefficient of 0.0240, with the highest zero-lift drag coefficient measured being slightly greater than twice the subsonic level.
2. Pitchup tendencies were noted for subsonic Mach numbers at relatively high lift coefficients.
3. Wing leading-edge droop increased the maximum lift-drag ratio approximately 8 percent at a Mach number of 0.80 but this effect was negligible at a Mach number of 0.90 and above.
4. The configuration exhibited stable lateral characteristics over the test Mach number range.

Langley Research Center,
National Aeronautics and Space Administration,
Langley Field, Va., December 1, 1959.

REFERENCES

1. Petynia, William W., Hasson, Dennis F., and Spooner, Stanley H.: Aerodynamic and Hydrodynamic Characteristics of a Proposed Supersonic Multijet Water-Based Hydro-Ski Aircraft With a Variable-Incidence Wing. NACA RM L57G05, 1957.
2. Bielat, Ralph P., Coffee, Claude W., Jr., and Petynia, William W.: Aerodynamic and Hydrodynamic Characteristics of a Deck-Inlet Multi-jet Water-Based-Aircraft Configuration Designed for Supersonic Flight. NACA RM L56H01, 1956.
3. Olson, Roland E., and Bielat, Ralph P.: An Aerodynamic and Hydrodynamic Investigation of Two Multijet Water-Based Aircraft Having Low Transonic Drag Rise. NACA RM L55Alla, 1955.
4. Whitcomb, Richard T.: A Study of the Zero-Lift Drag-Rise Characteristics of Wing-Body Combinations Near the Speed of Sound. NACA Rep. 1273, 1956. (Supersedes NACA RM L52H08.)
5. Whitcomb, Richard T., and Fischetti, Thomas L.: Development of a Supersonic Area Rule and an Application to the Design of a Wing-Body Combination Having High Lift-to-Drag Ratios. NACA RM L53H31a, 1953.
6. Whitcomb, Richard T.: Some Considerations Regarding the Application of the Supersonic Area Rule to the Design of Airplane Fuselages. NACA RM L56E23a, 1956.
7. Coffee, Claude W., Jr.: Hydrodynamic Characteristics of a Model of a Proposed Six-Engine Hull-Type Seaplane Designed for Supersonic Flight. NACA RM L58E13, 1958.
8. Lindsey, W. F., Daley, Bernard N., and Humphreys, Milton D.: The Flow and Force Characteristics of Supersonic Airfoils at High Subsonic Speeds. NACA TN 1211, 1947.

TABLE I.- PERTINENT CHARACTERISTICS AND DIMENSIONS
OF THE FULL-SIZE SIX-ENGINE SHIPPLANE

General:

Gross weight, lb	220,000
Wing area, sq ft	1,835
Engines, Orenda Iroquois PS-13	6
Takeoff thrust (without afterburners), lb	120,000
Wing loading, lb/sq ft	120
Takeoff thrust-weight ratio	0.545

Wing:

Span, ft	74.2
Airfoil section	Biconvex
Thickness, percent chord	3.5
Aspect ratio	3.0
Taper ratio	0.333
Sweepback (0.25c), deg	20.17
Sweepback (0.80c), deg	0
Incidence (wing root to base line), deg	3
Geometric twist, deg	0
Dihedral, deg	0
Root chord, ft	37.16
Mean aerodynamic chord, ft	26.82
Tip chord, ft	12.33

Hull:

Length, overall, ft	134.09
Beam at chines, maximum ft	9.2
Height, maximum including hull nacelles, ft	15

Horizontal tail:

Span, ft	32.7
Airfoil section	Biconvex
Thickness, percent chord	3.5
Area, sq ft	355
Aspect ratio	3.0
Taper ratio	0.4
Sweepback (0.25c), deg	17.3
Sweepback (0.80c), deg	0
Dihedral, deg	15
Tail length (from 0.25 wing 6 to 0.25 tail 6 parallel to wing root chord), ft	65.08

Vertical tail:

Airfoil section	NACA 64A006
Area, sq ft	242.6
Aspect ratio	1.1
Sweepback (0.25c), deg	50

Area curves:

Mach number, 1.0	
Maximum cross-sectional area, sq ft	157.5
Maximum diameter of equivalent body, ft	14.2
Length, ft	134.1
Fineness ratio of equivalent body	9.5
Mach number, 1.8	
Maximum cross-sectional area, sq ft	135.0
Maximum diameter of equivalent body, ft	13.1
Length, ft	134.1
Fineness ratio of equivalent body	10.2
Total surface area, sq ft	9,980

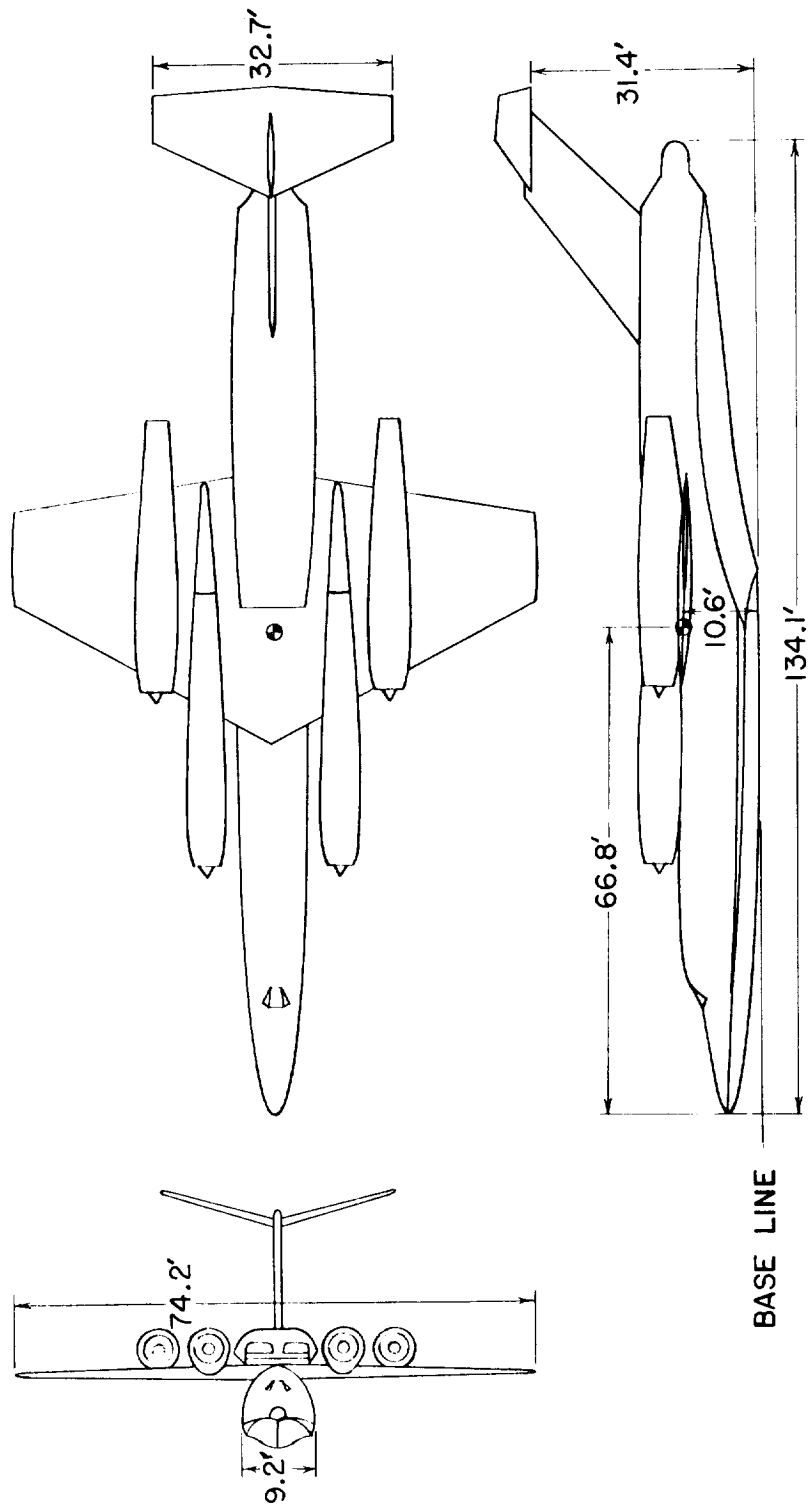


Figure 1.- General arrangement of the six-engine hull-type seaplane.

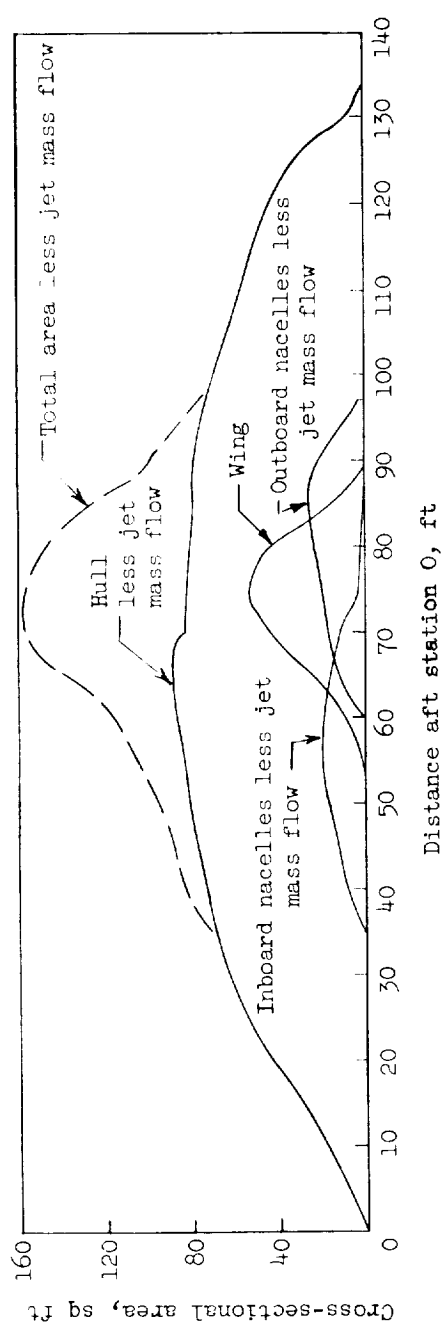
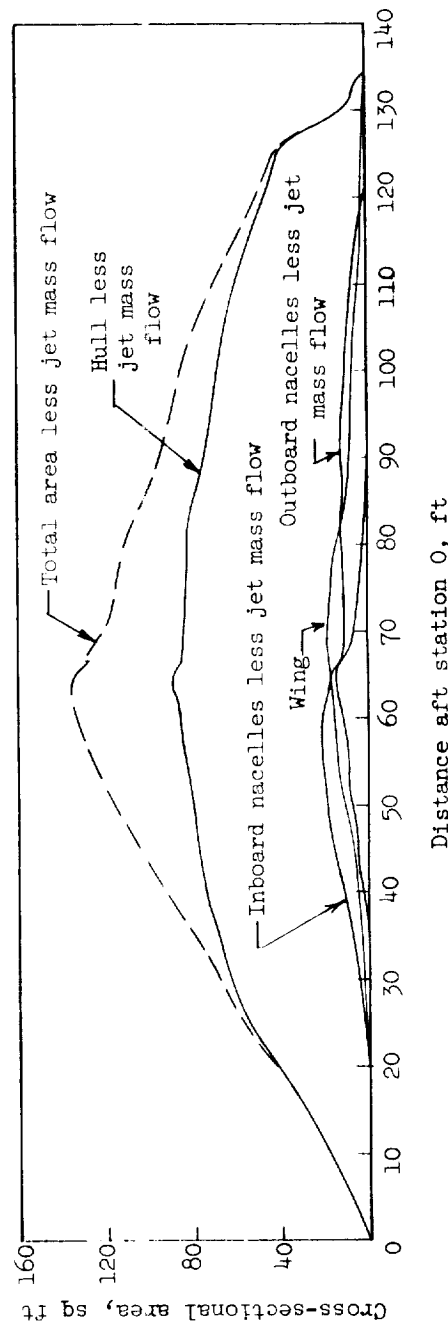
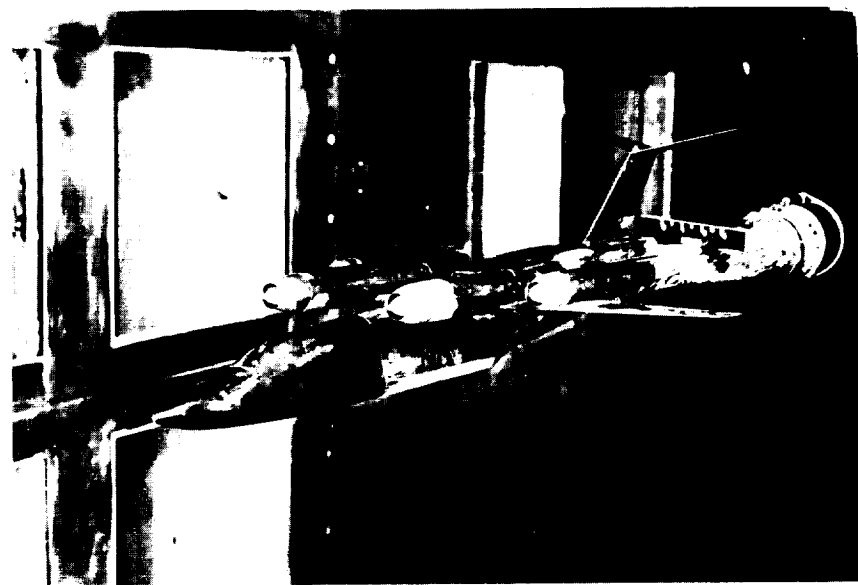
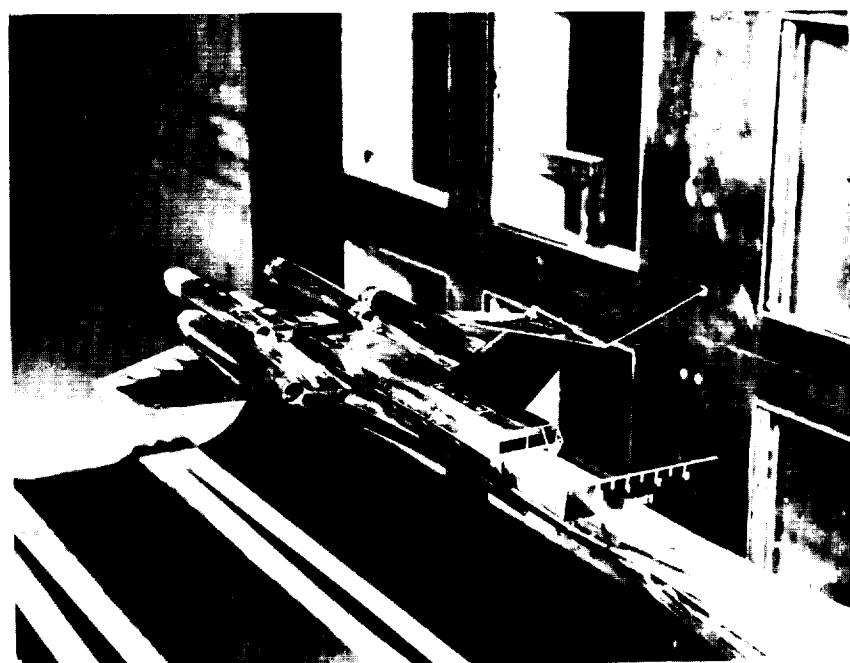
(a) $M = 1.0.$ (b) $M = 1.8.$

Figure 2.- Cross-sectional area curves.



L-58-1956



L-58-1957

Figure 3.- The 0.02-scale model of the six-engine configuration mounted in the Langley 8-foot transonic pressure tunnel.

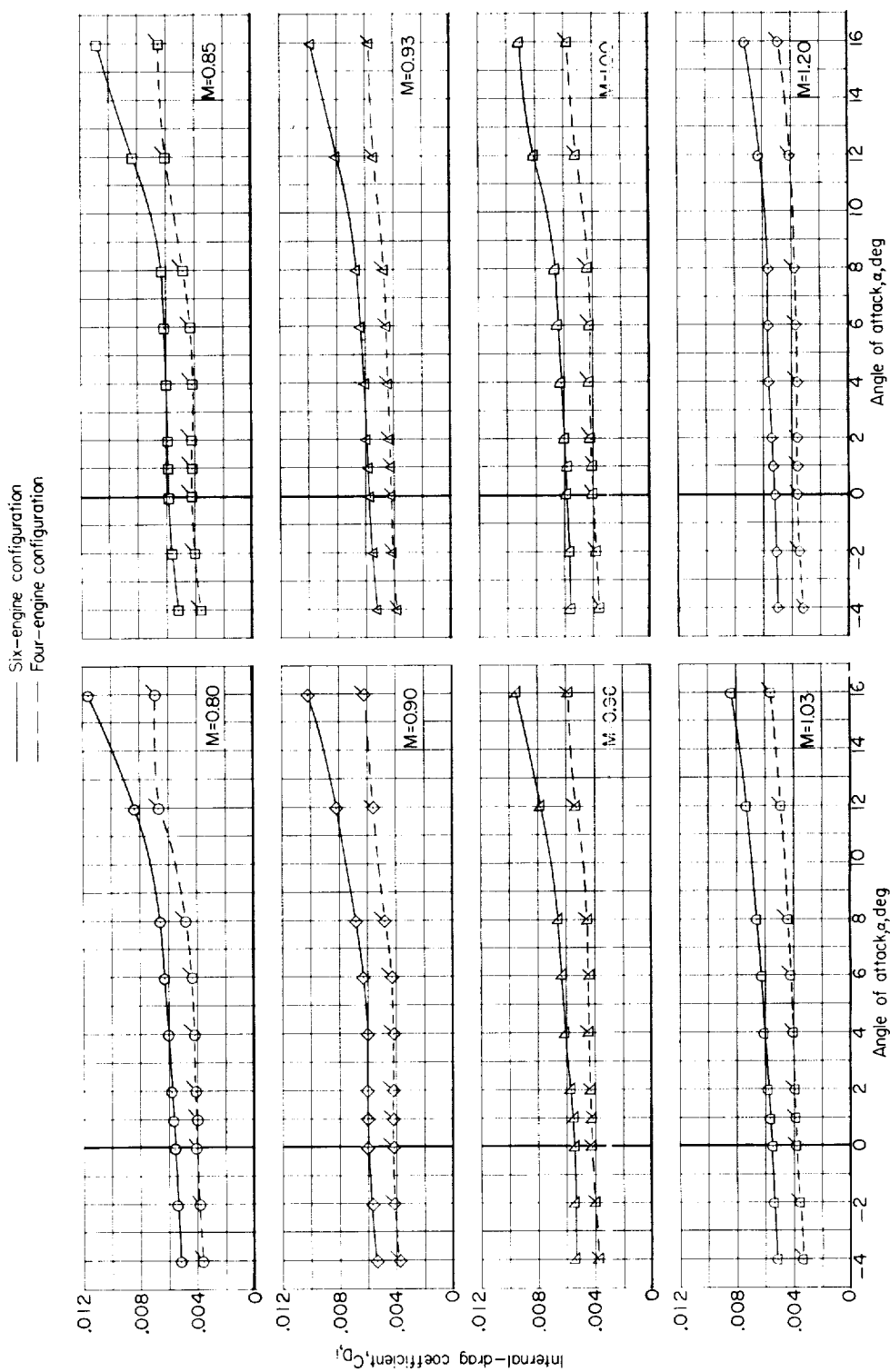


Figure 4.- Variation of total internal-drag coefficient with angle of attack for the six- and four-engine configurations. $\beta = 0^\circ$; $i_t = 20^\circ$.

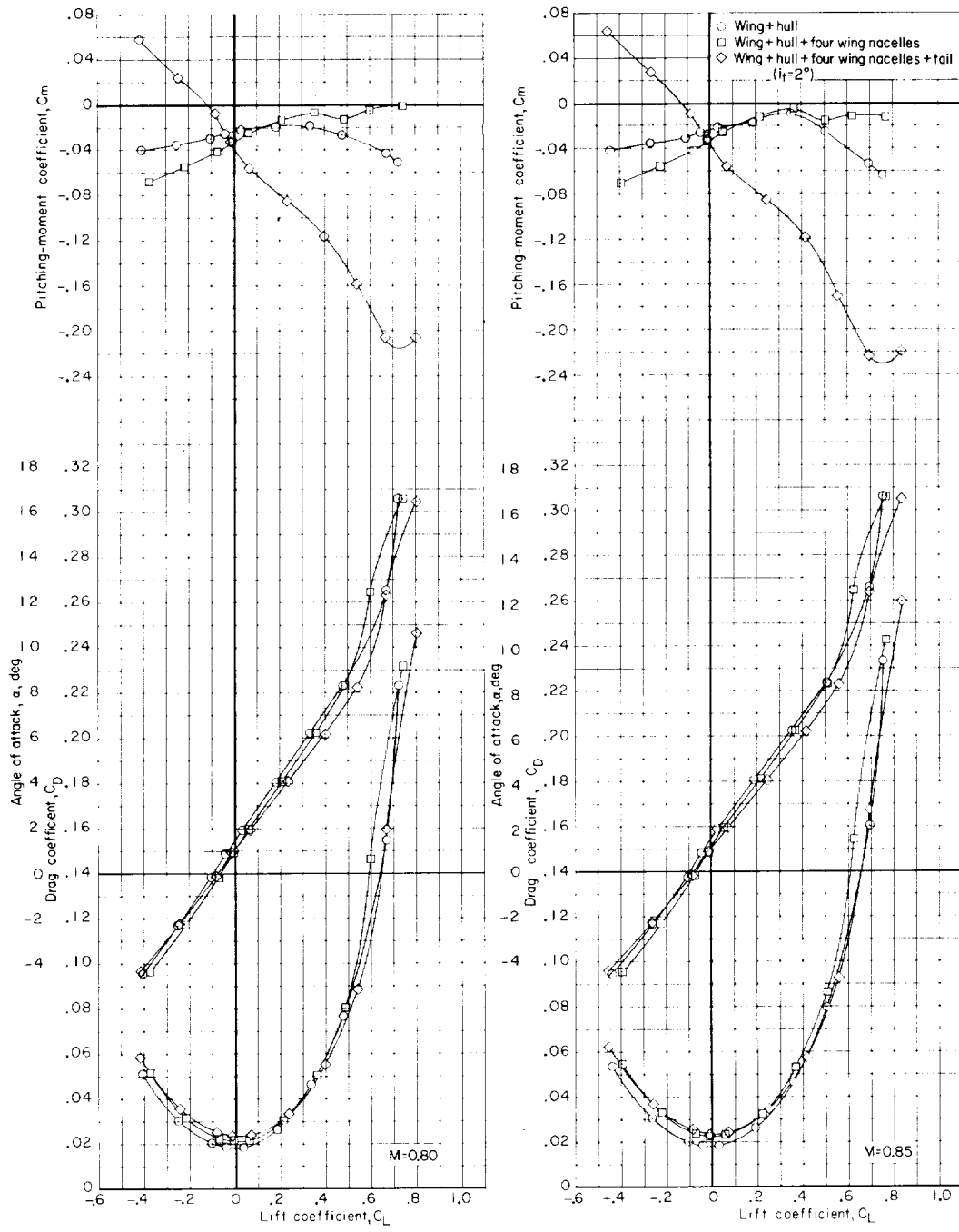
(a) $M = 0.80$ and 0.85 .

Figure 5.- Longitudinal aerodynamic characteristics of the six-engine configurations.

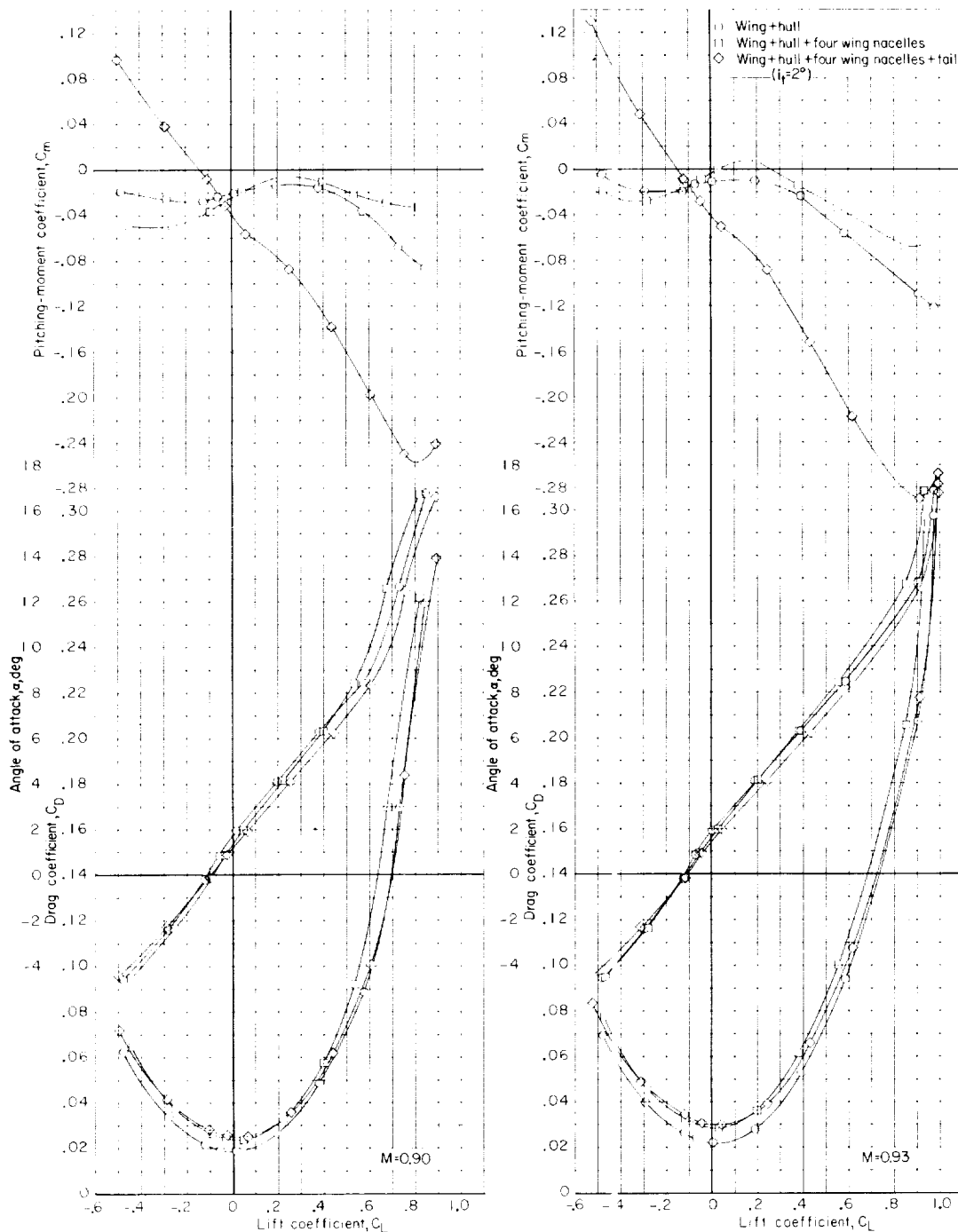
(b) $M = 0.90$ and 0.93 .

Figure 5.- Continued.

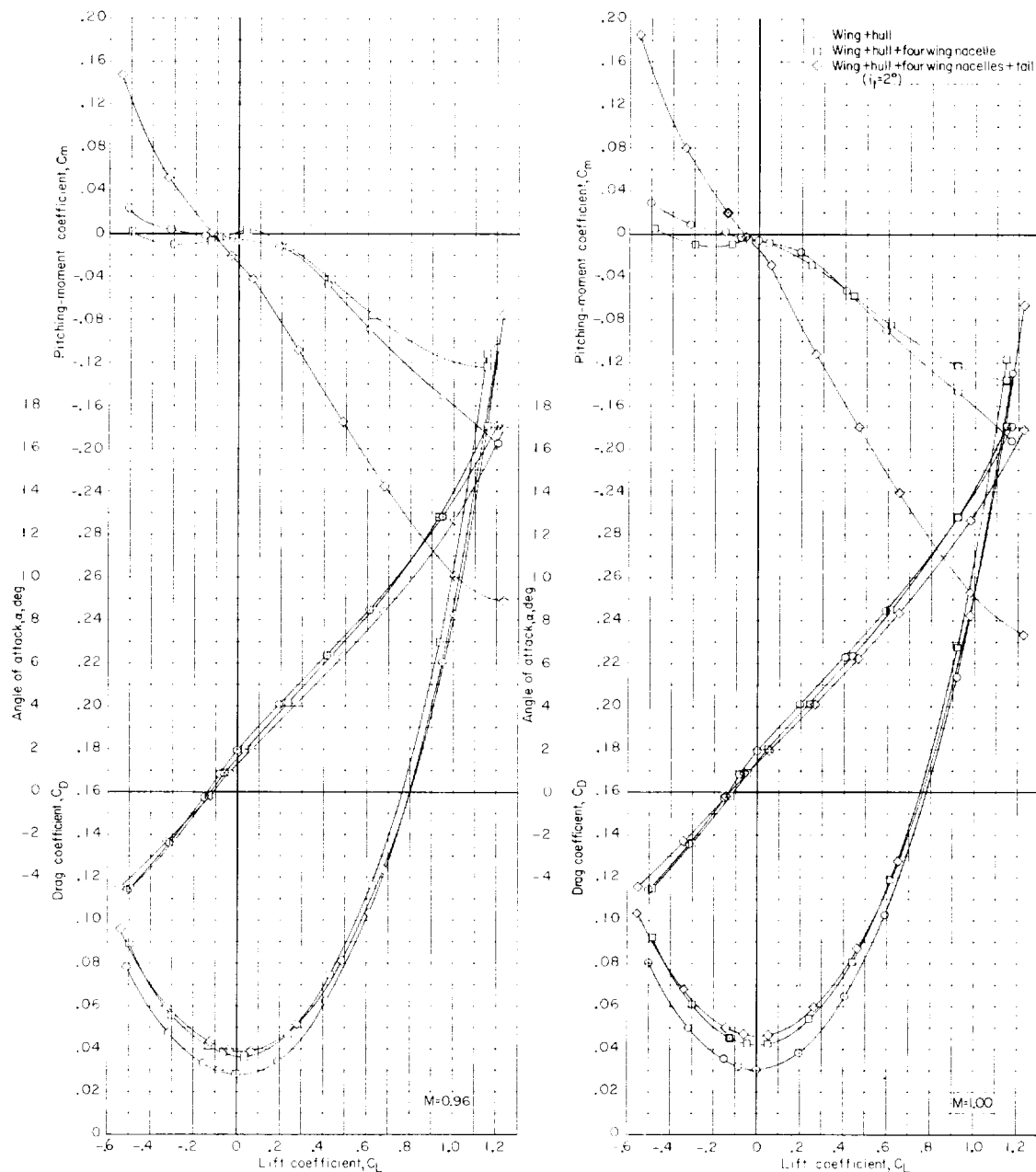
(c) $M = 0.96$ and 1.00 .

Figure 5.- Continued.

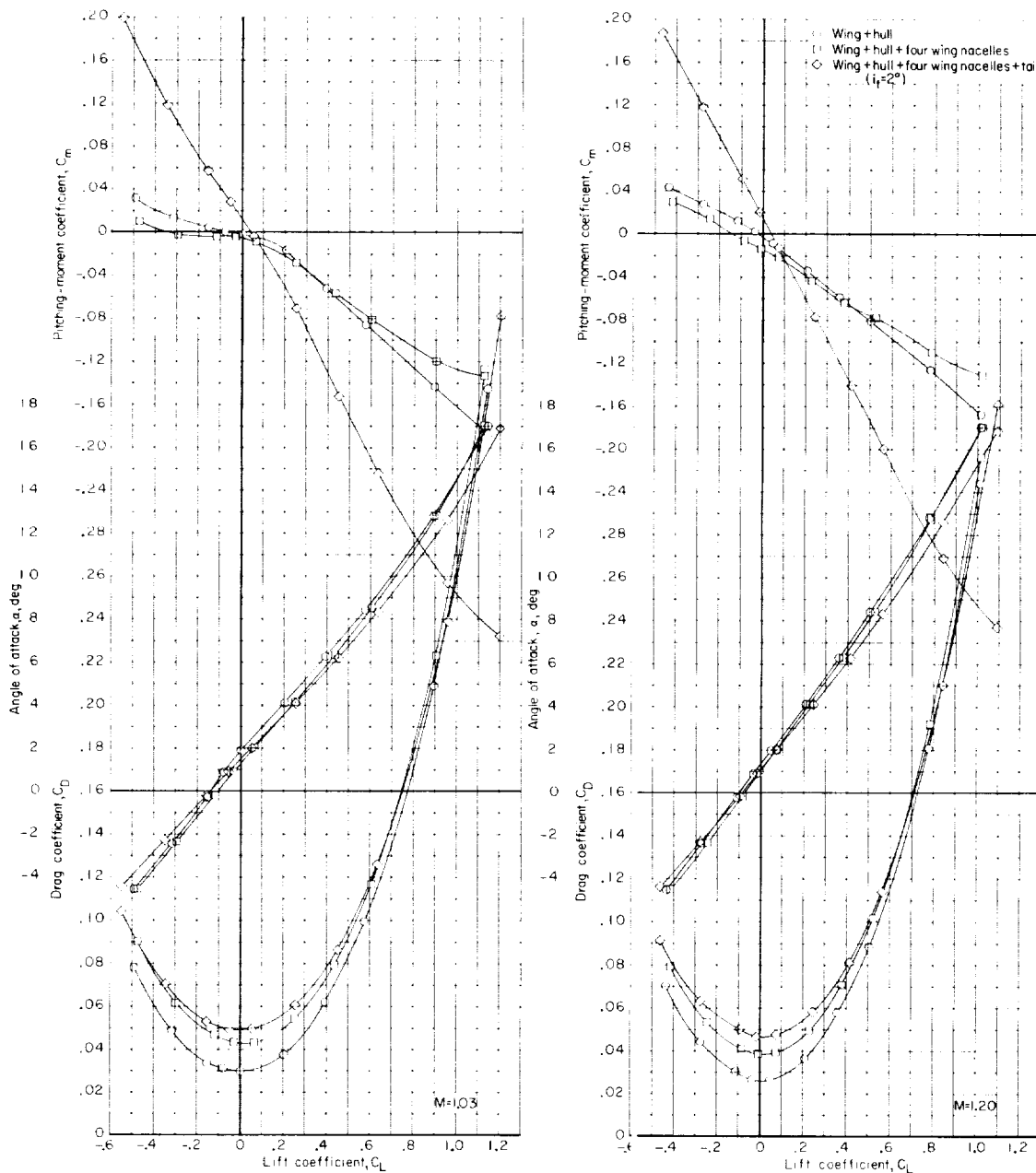


Figure 5.- Concluded.

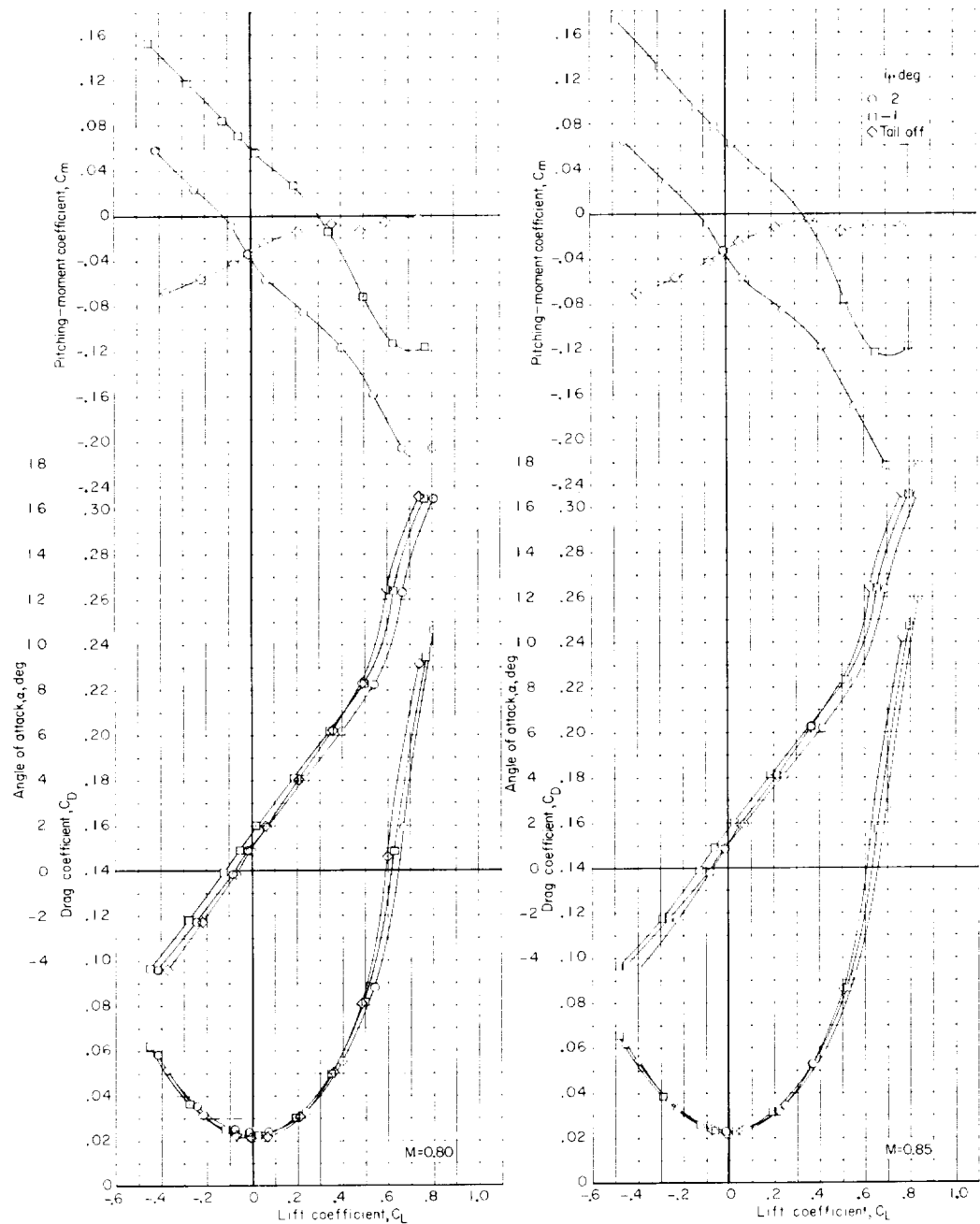
(a) $M = 0.80$ and 0.85 .

Figure 6.- Effect of stabilizer incidence on the longitudinal aerodynamic characteristics of the six-engine configuration.

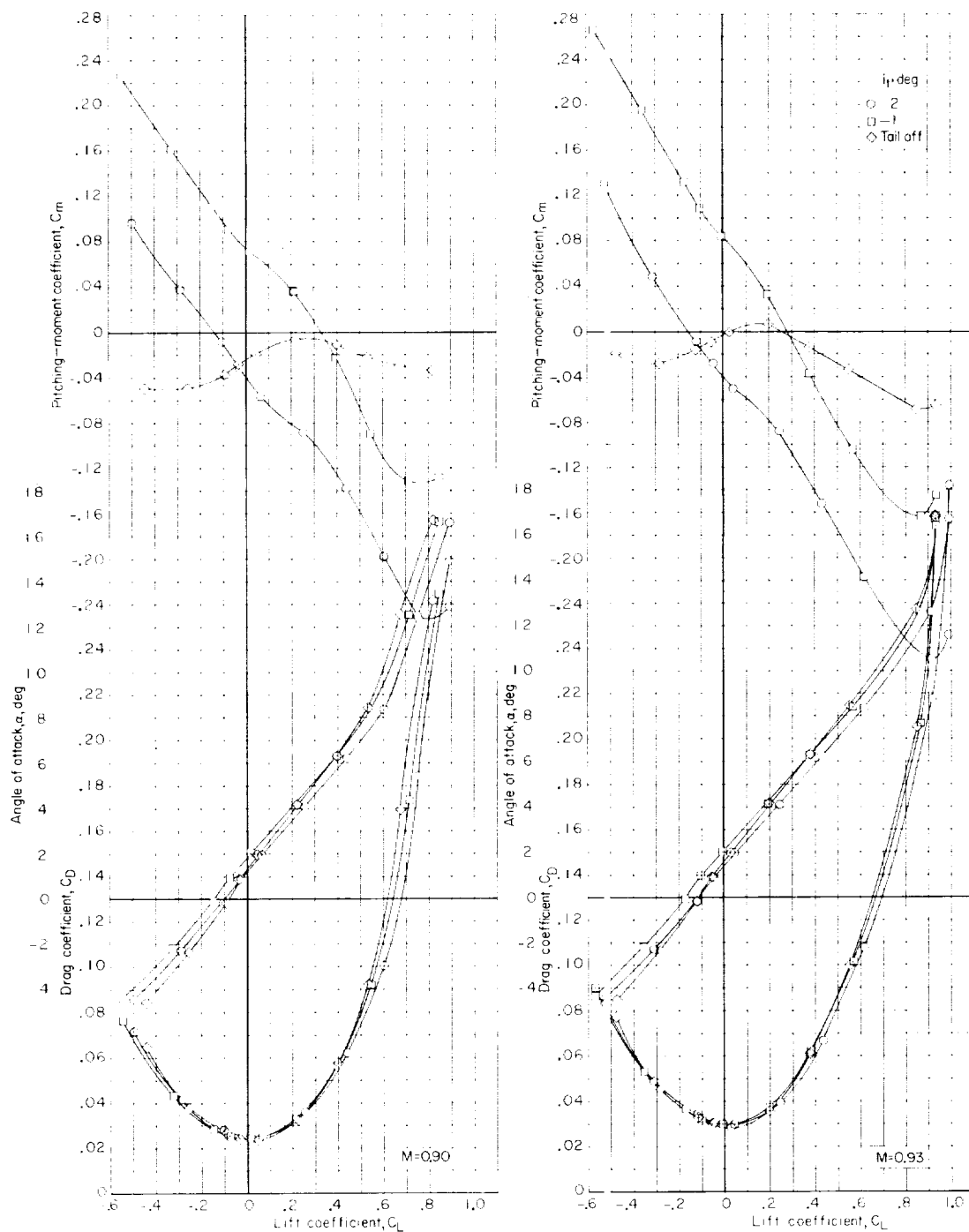
(b) $M = 0.90$ and 0.93 .

Figure 6.- Continued.

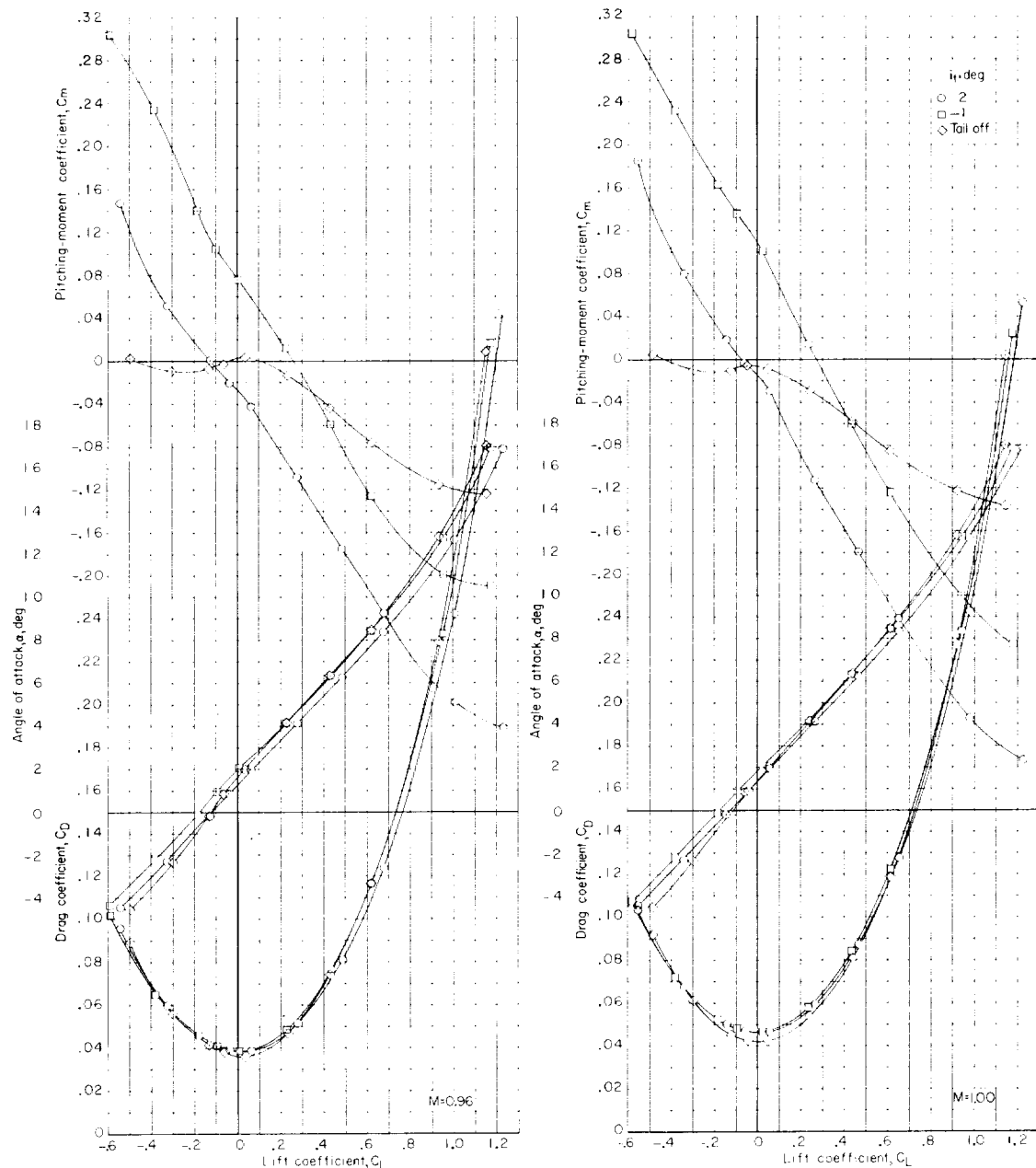
(c) $M = 0.96$ and 1.00.

Figure 6.- Continued.

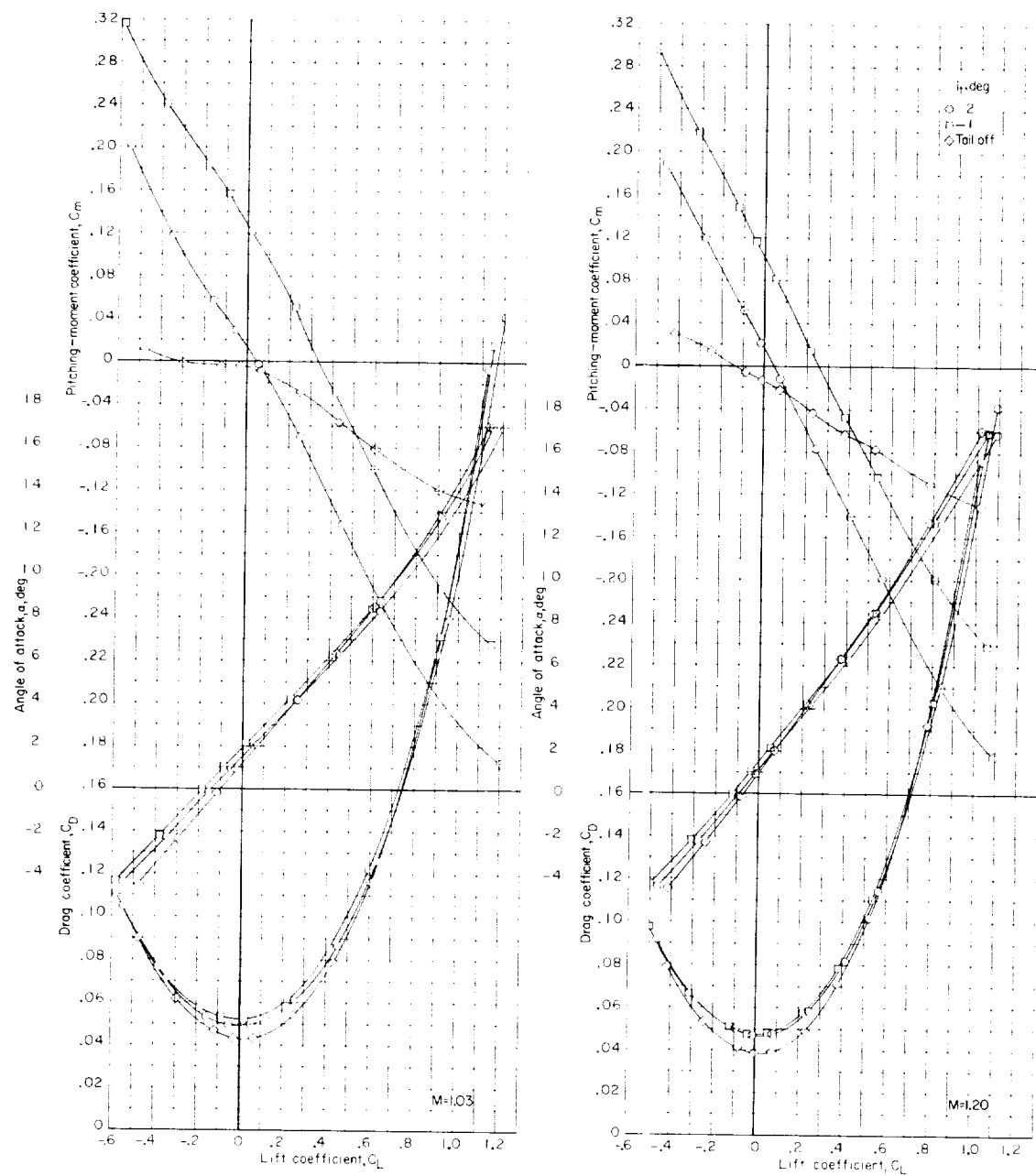
(d) $M = 1.03$ and 1.20 .

Figure 6.- Concluded.

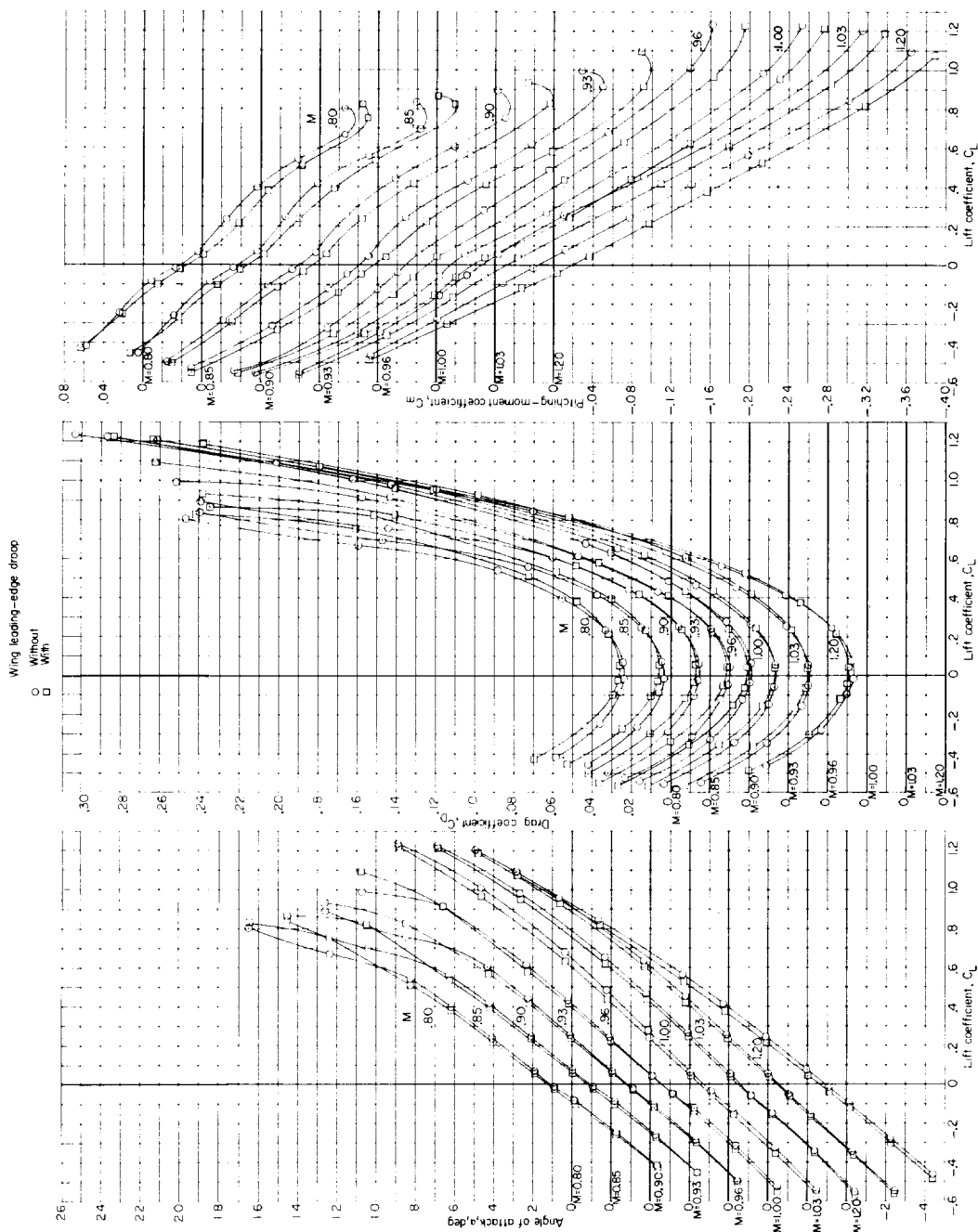


Figure 7.- Effect of wing leading-edge droop on the longitudinal aerodynamic characteristics of the six-engine configuration. $It = 20$.

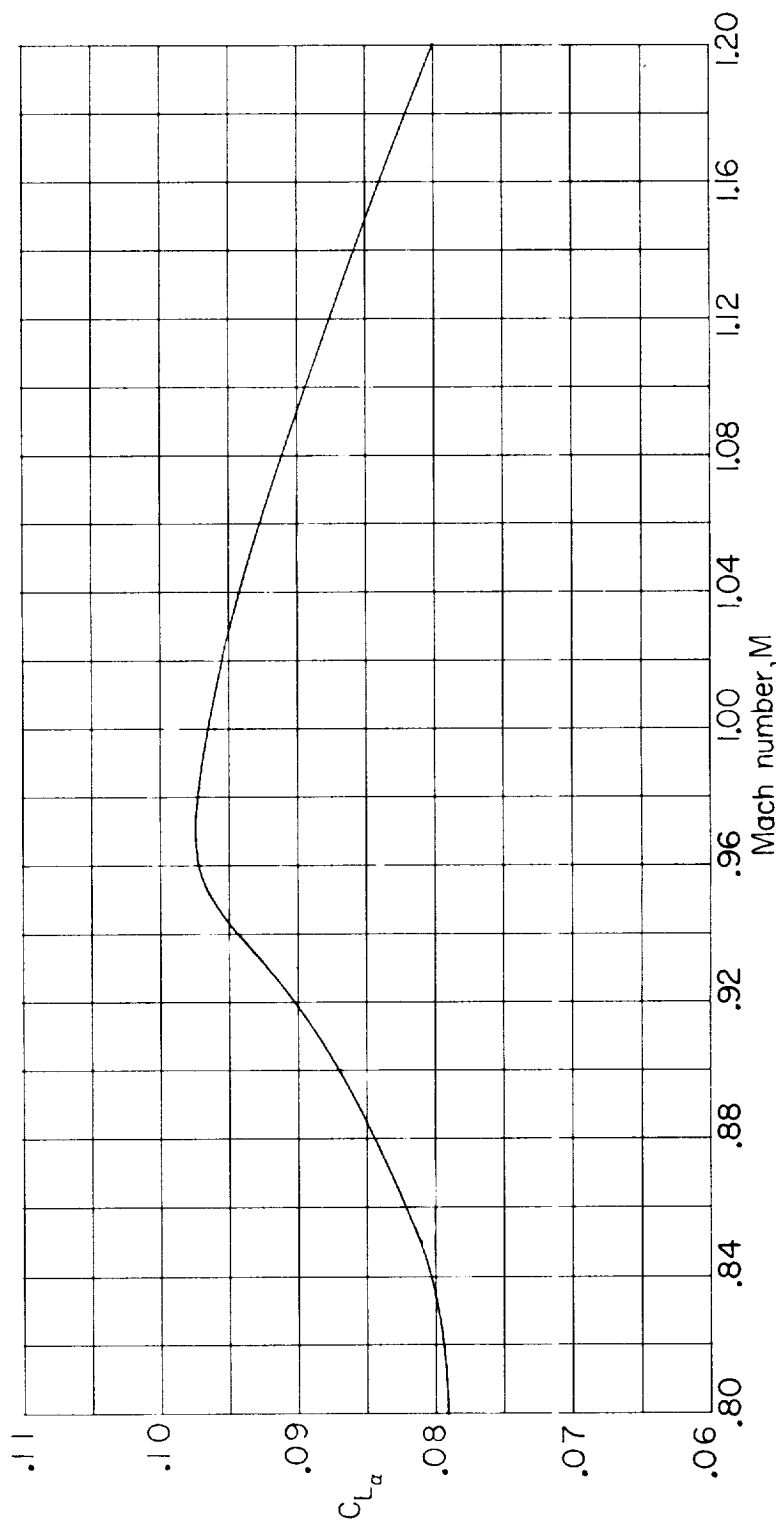


Figure 8.- Variation with Mach number of the lift-curve slope for the six-engine configuration.
 $i_t = 2^{\circ}$.

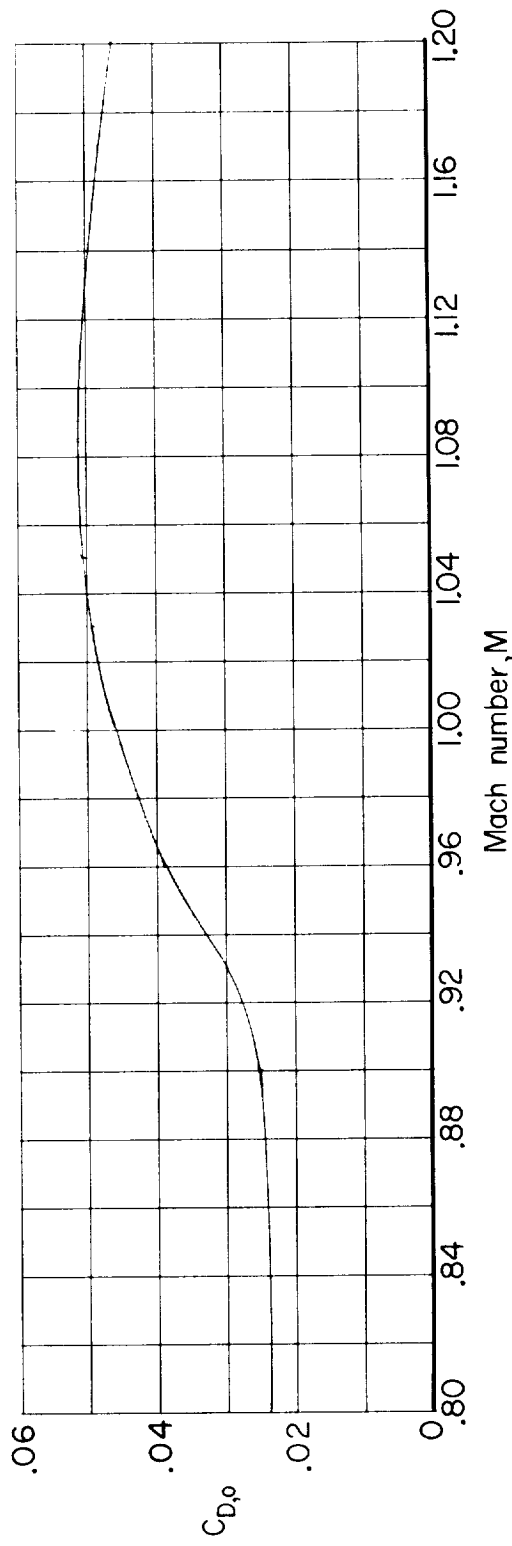


Figure 9.- Variation with Mach number of the zero-lift drag coefficient for the six-engine configuration. $\alpha_t = 20^\circ$.

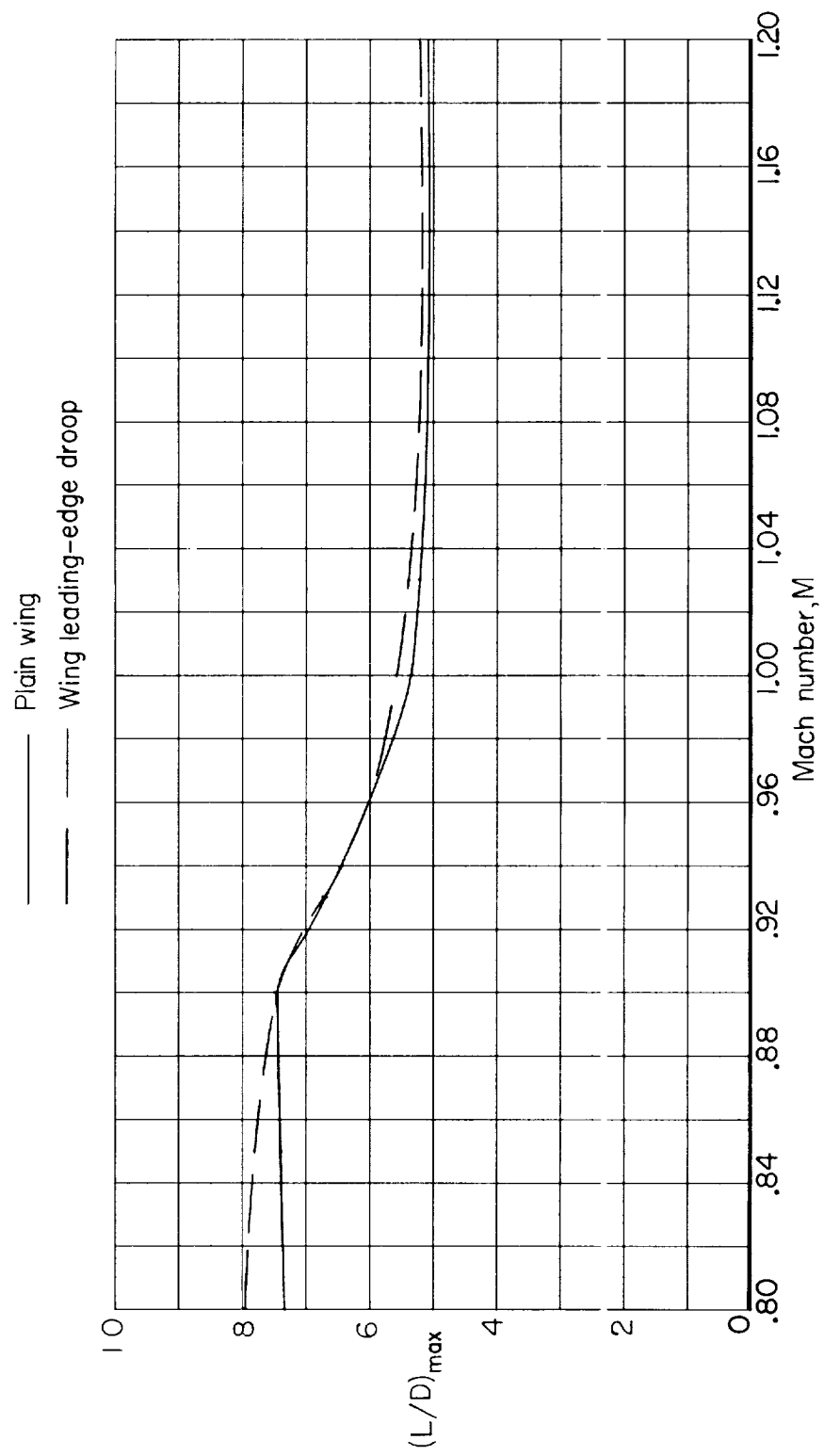


Figure 10.- Effect of wing leading-edge droop on the maximum lift-drag ratio of the six-engine configuration. $i_t = 2^\circ$.

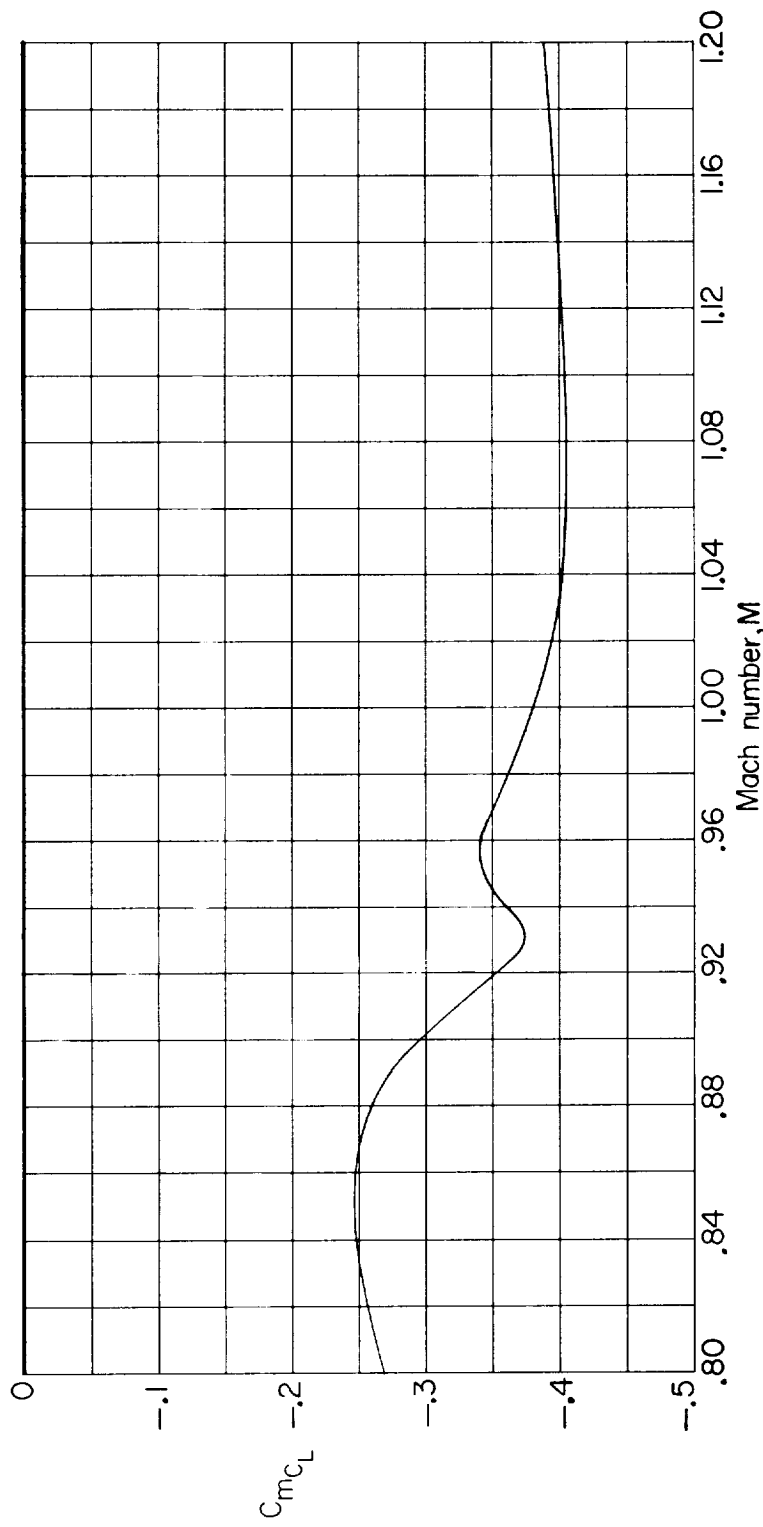


Figure 11.- Variation with Mach number of the static-longitudinal-stability parameter for the six-engine configuration. $\alpha_t = -1^\circ$; $C_L = 0.3$.

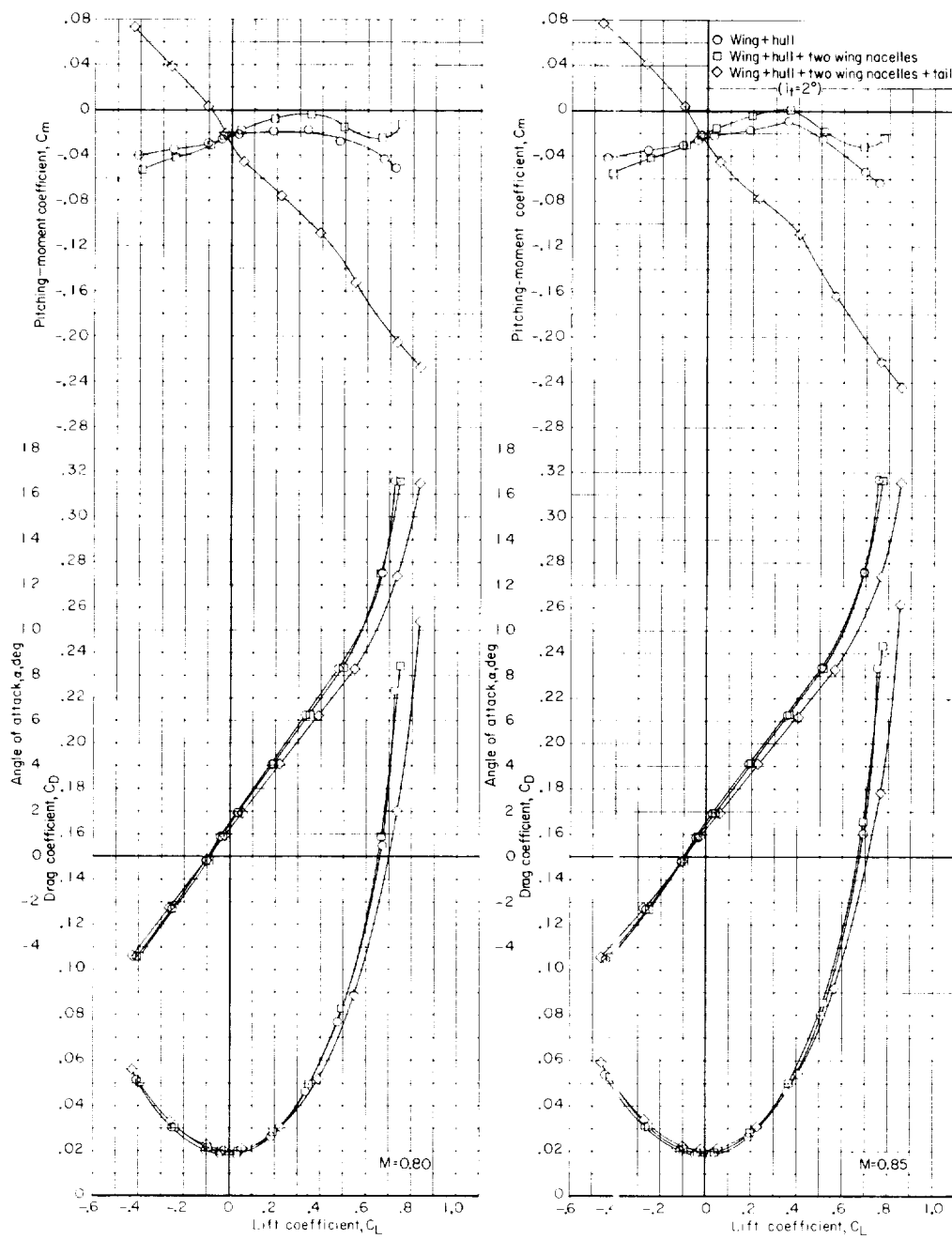
(a) $M = 0.80$ and 0.85 .

Figure 12.- Longitudinal aerodynamic characteristics of the four-engine configurations.

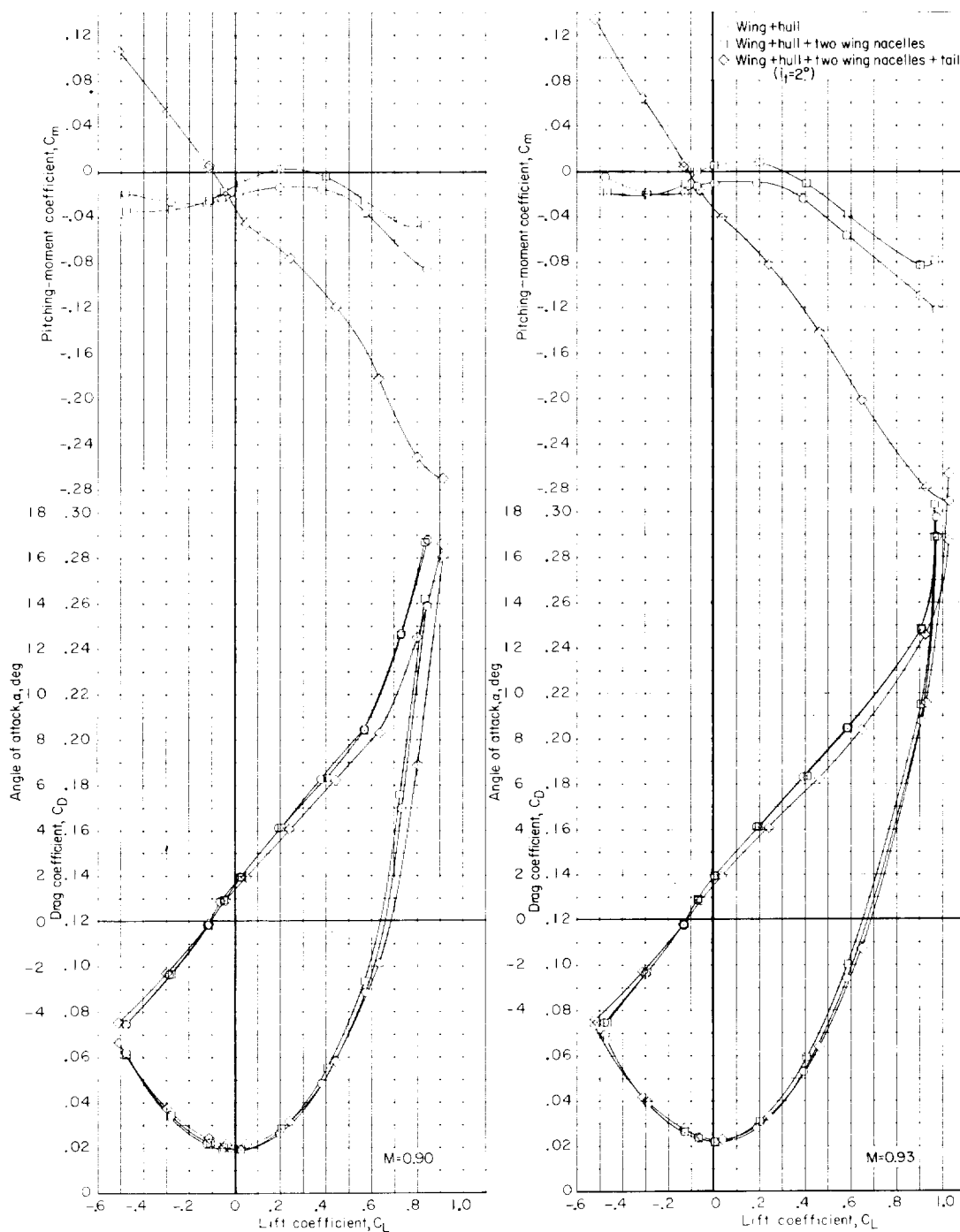


Figure 12.- Continued.

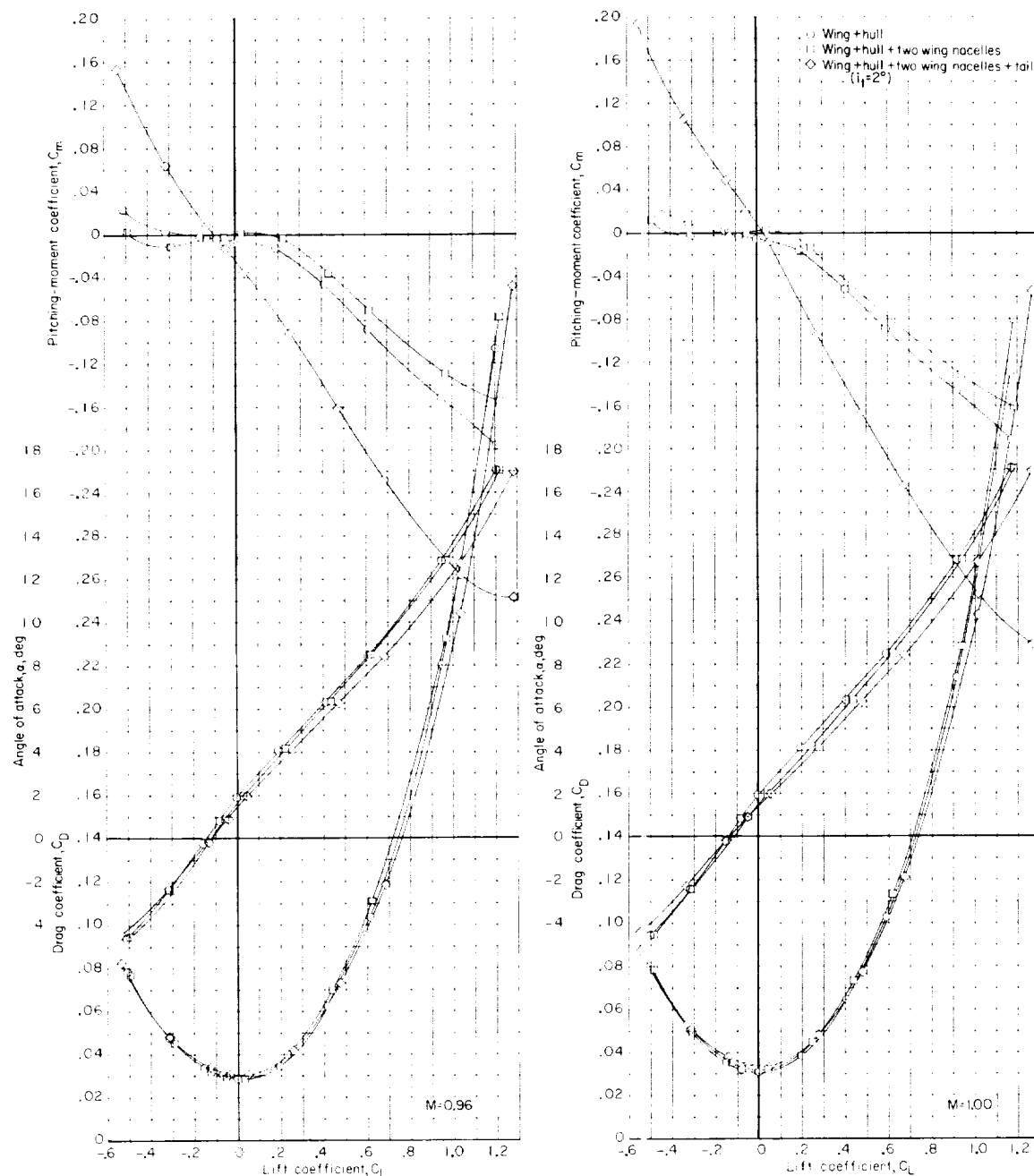
(c) $M = 0.96$ and 1.00 .

Figure 12.- Continued.

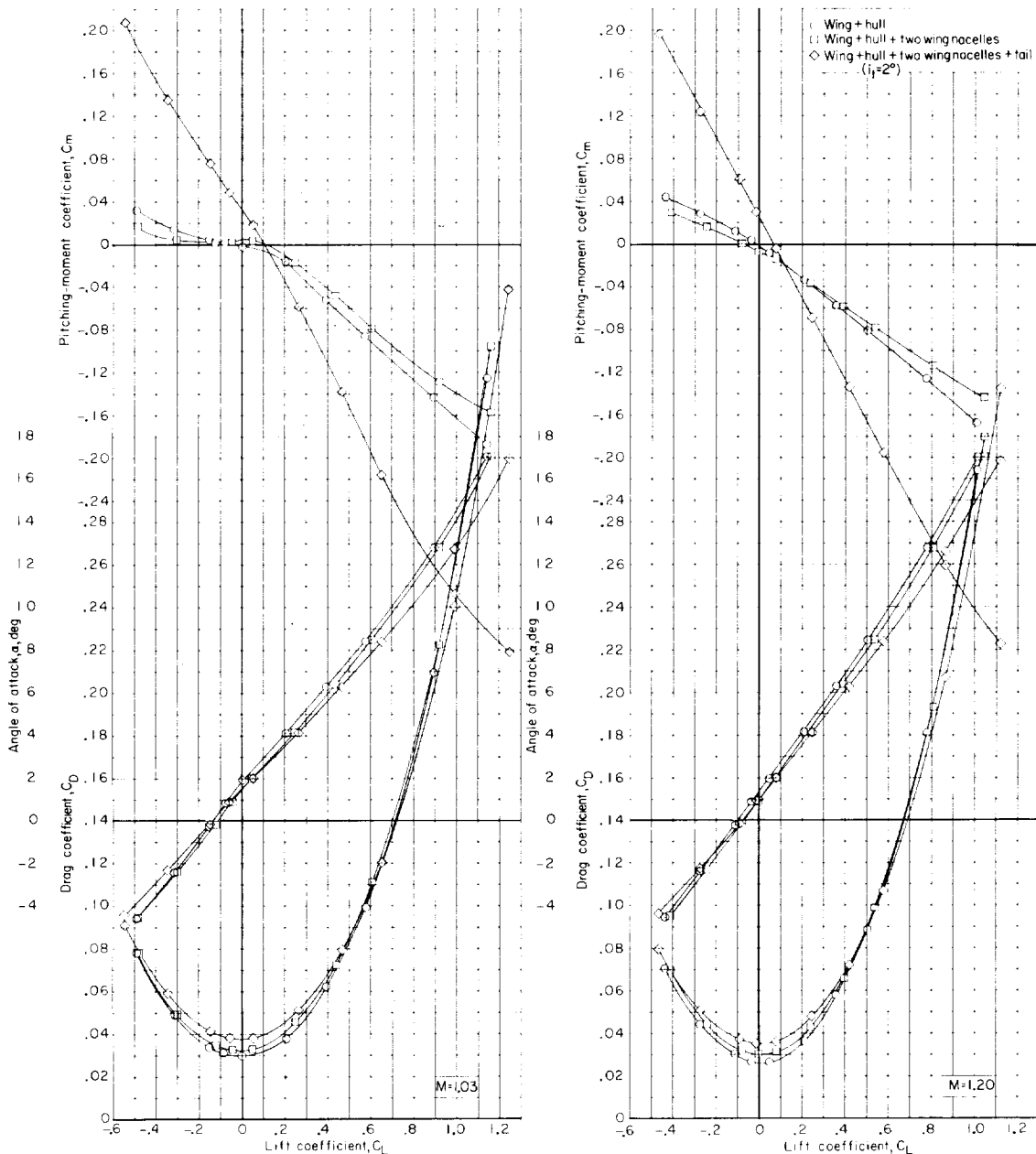
(d) $M = 1.03$ and 1.20 .

Figure 12.- Concluded.

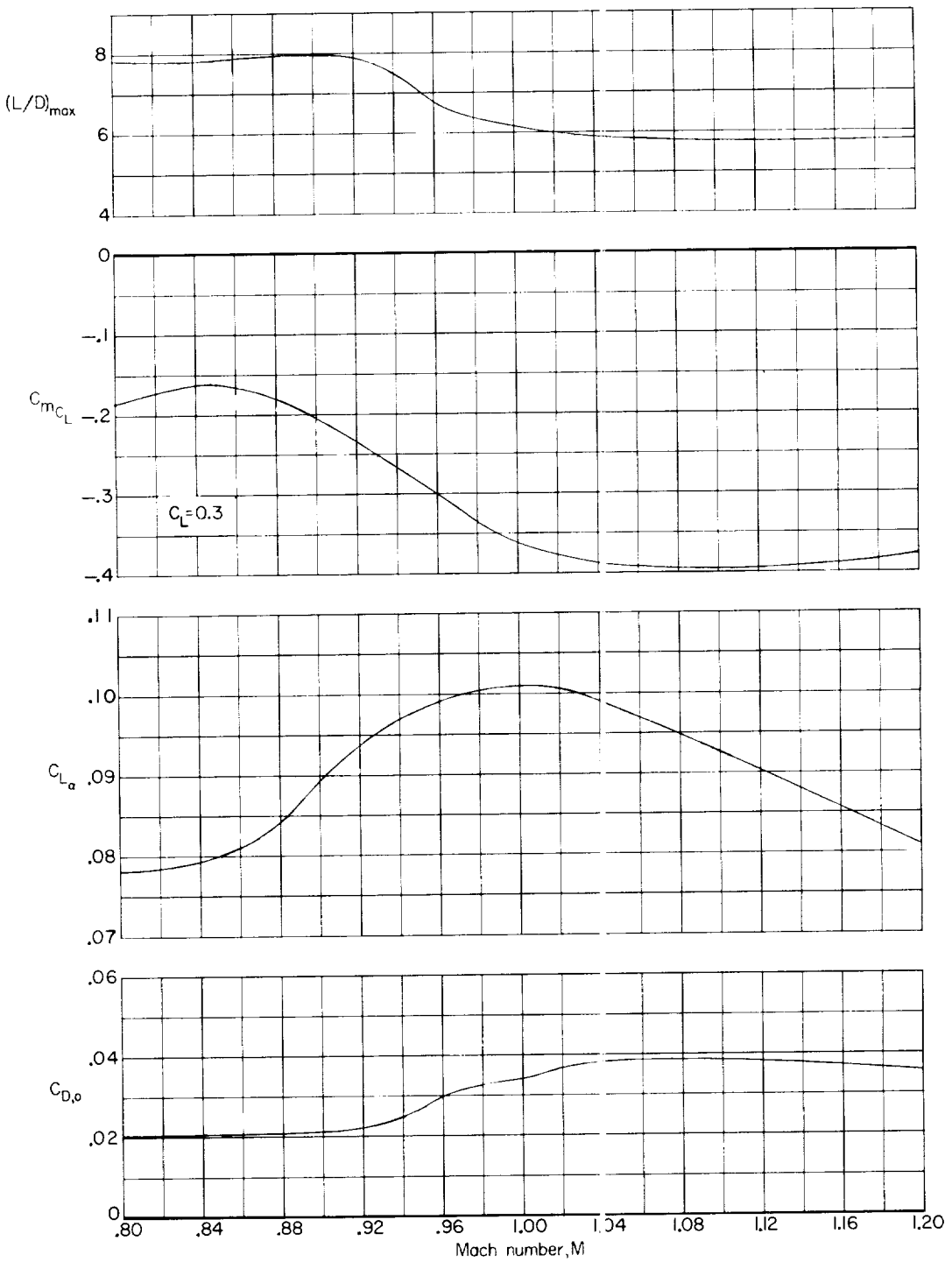


Figure 13.- Longitudinal aerodynamic characteristics of the four-engine configuration. $i_t = 2^\circ$.

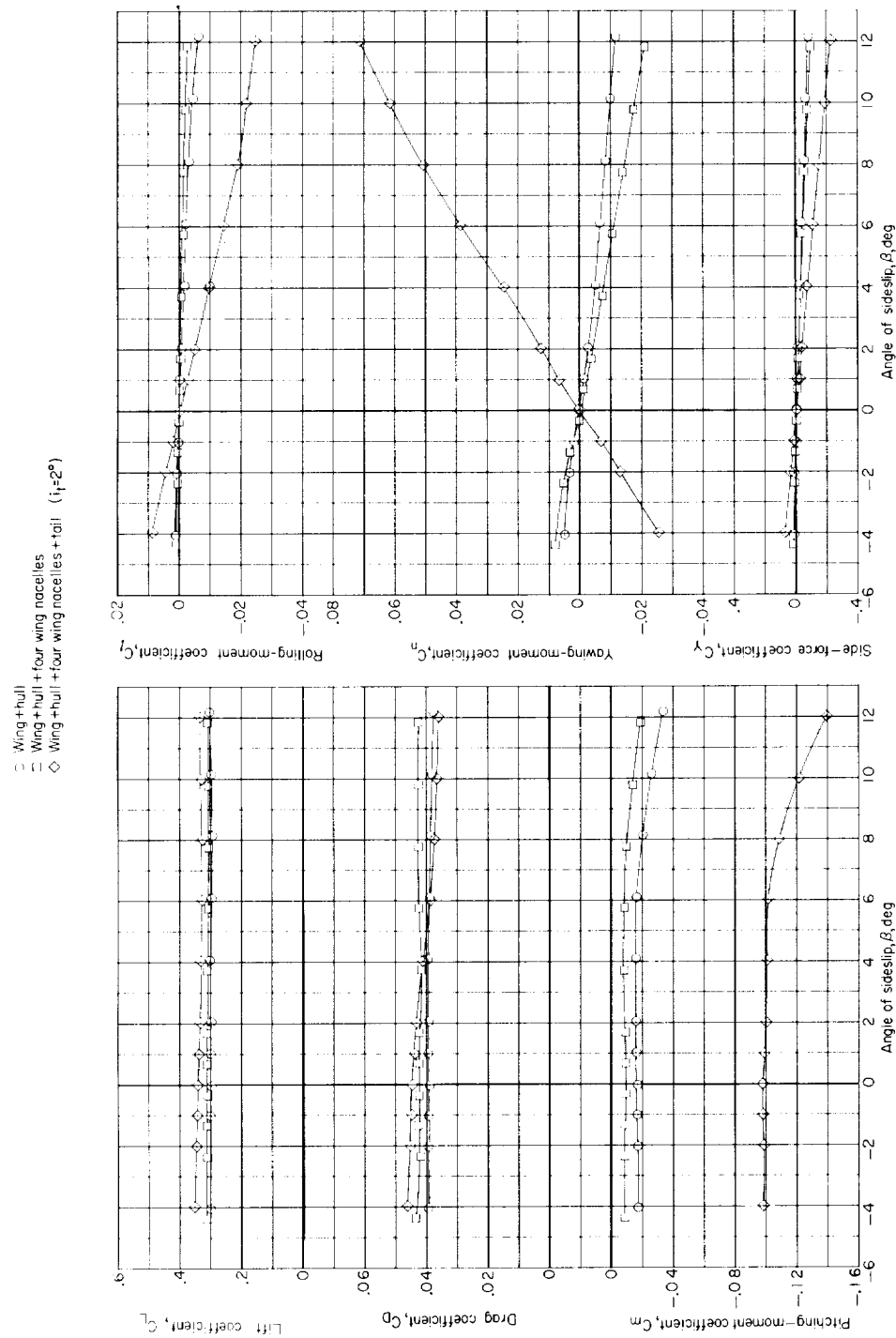
(a) $M = 0.80$.

Figure 14.- Variation with angle of sideslip of the aerodynamic characteristics of the six-engine configurations. $\alpha \approx 5.7^\circ$.

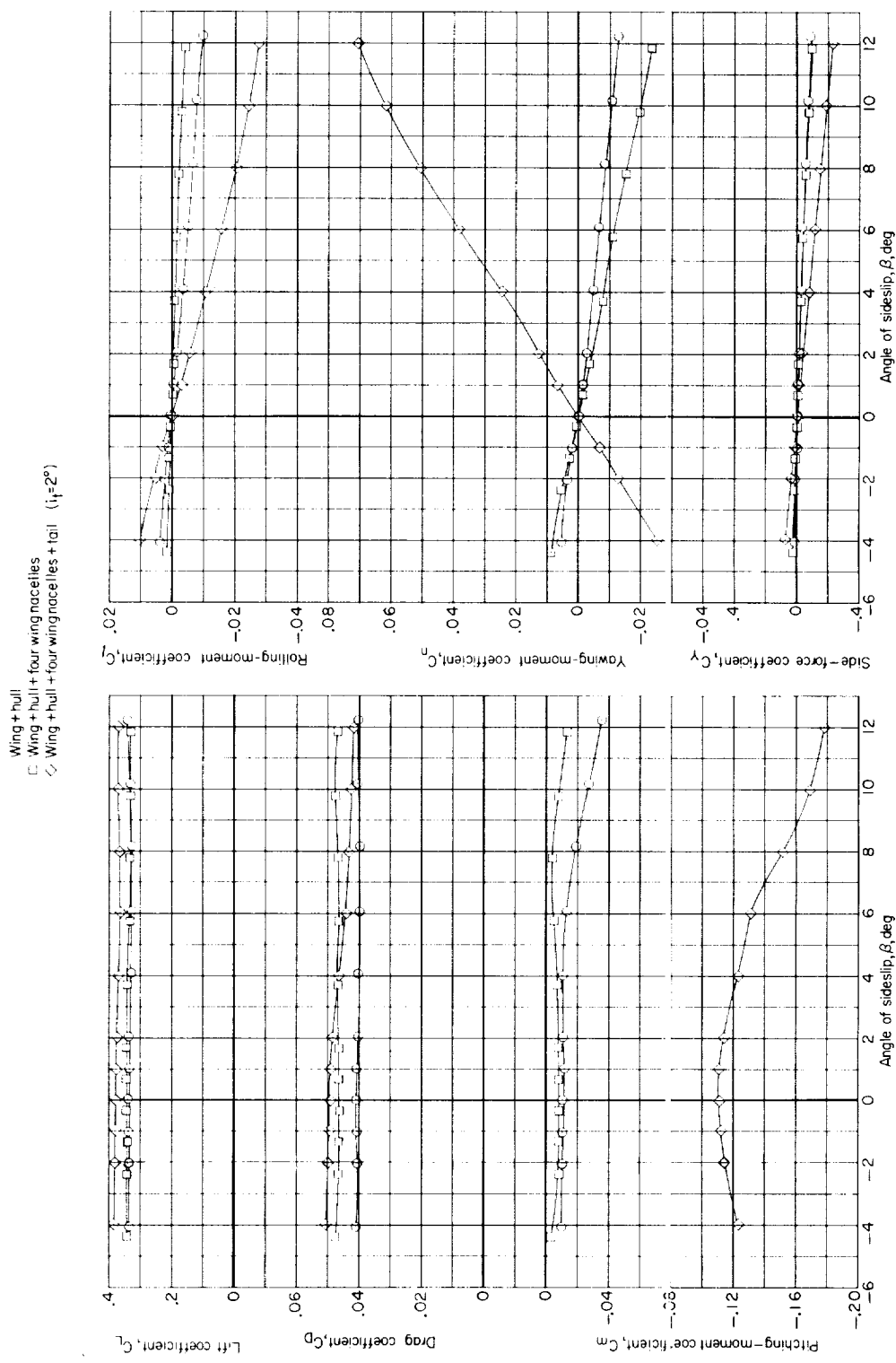
(b) $M = 0.90$.

Figure 14.- Continued.

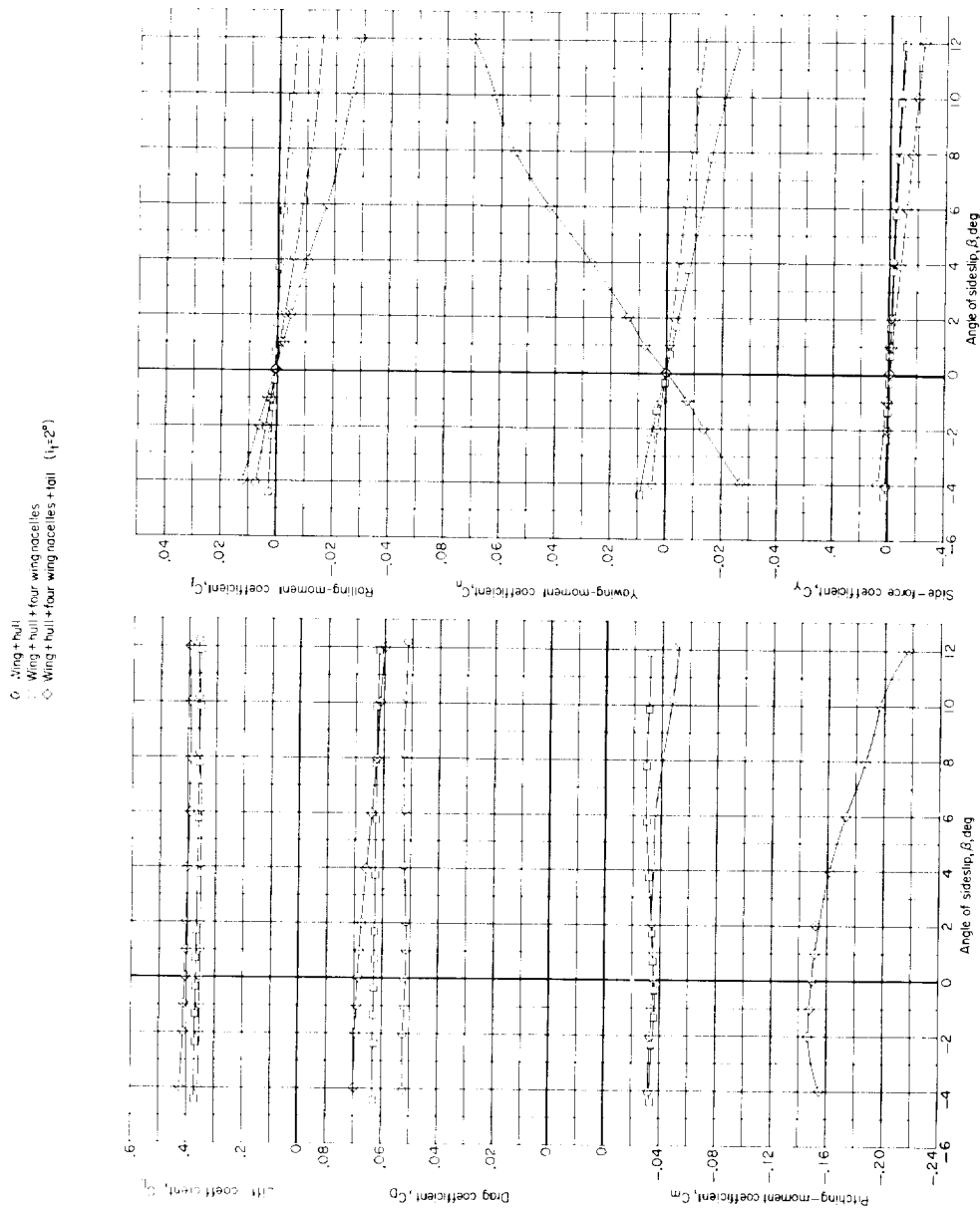
(c) $M = 0.96$.

Figure 14.- Continued.

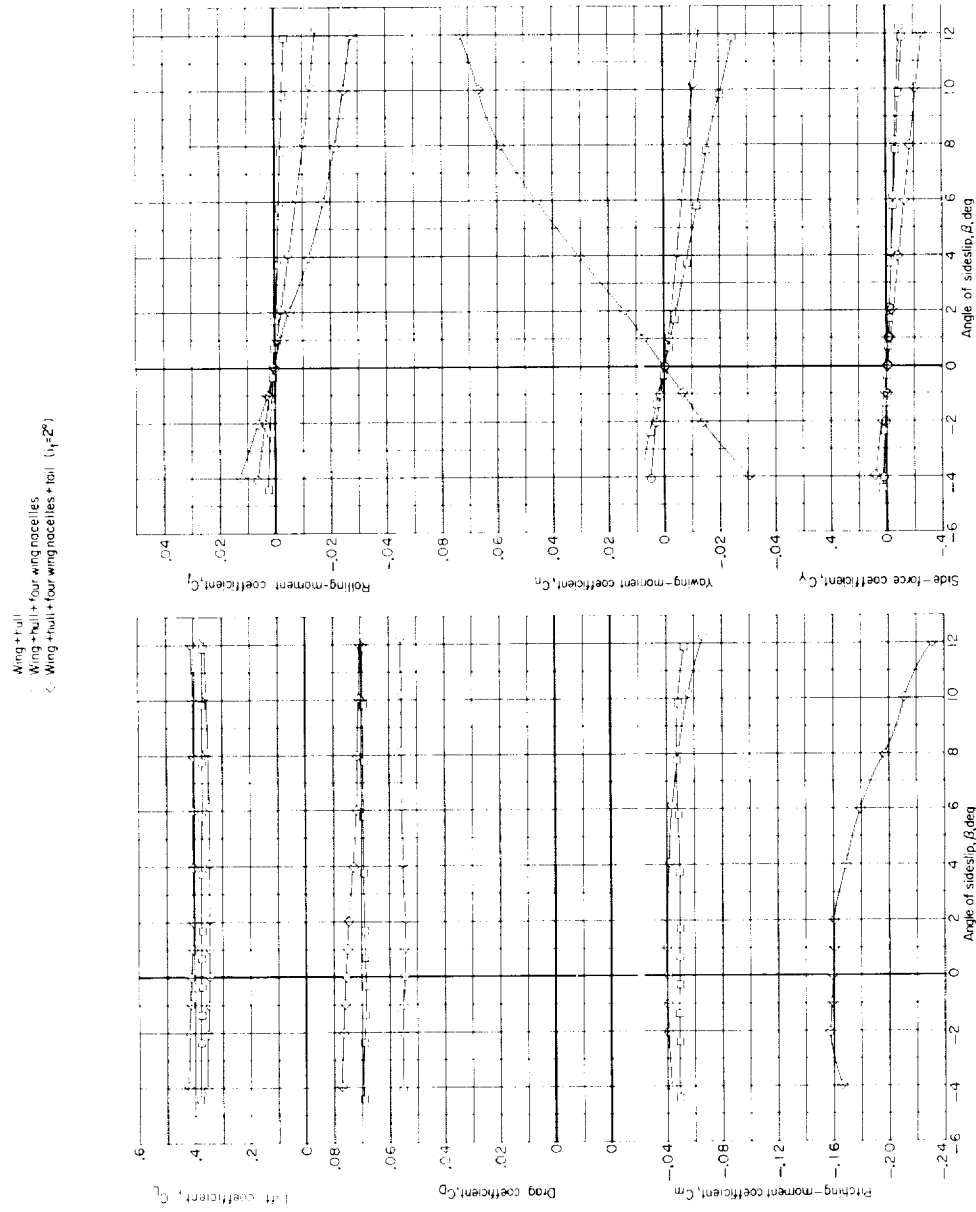
(d) $M = 1.00$.

Figure 14.- Continued.

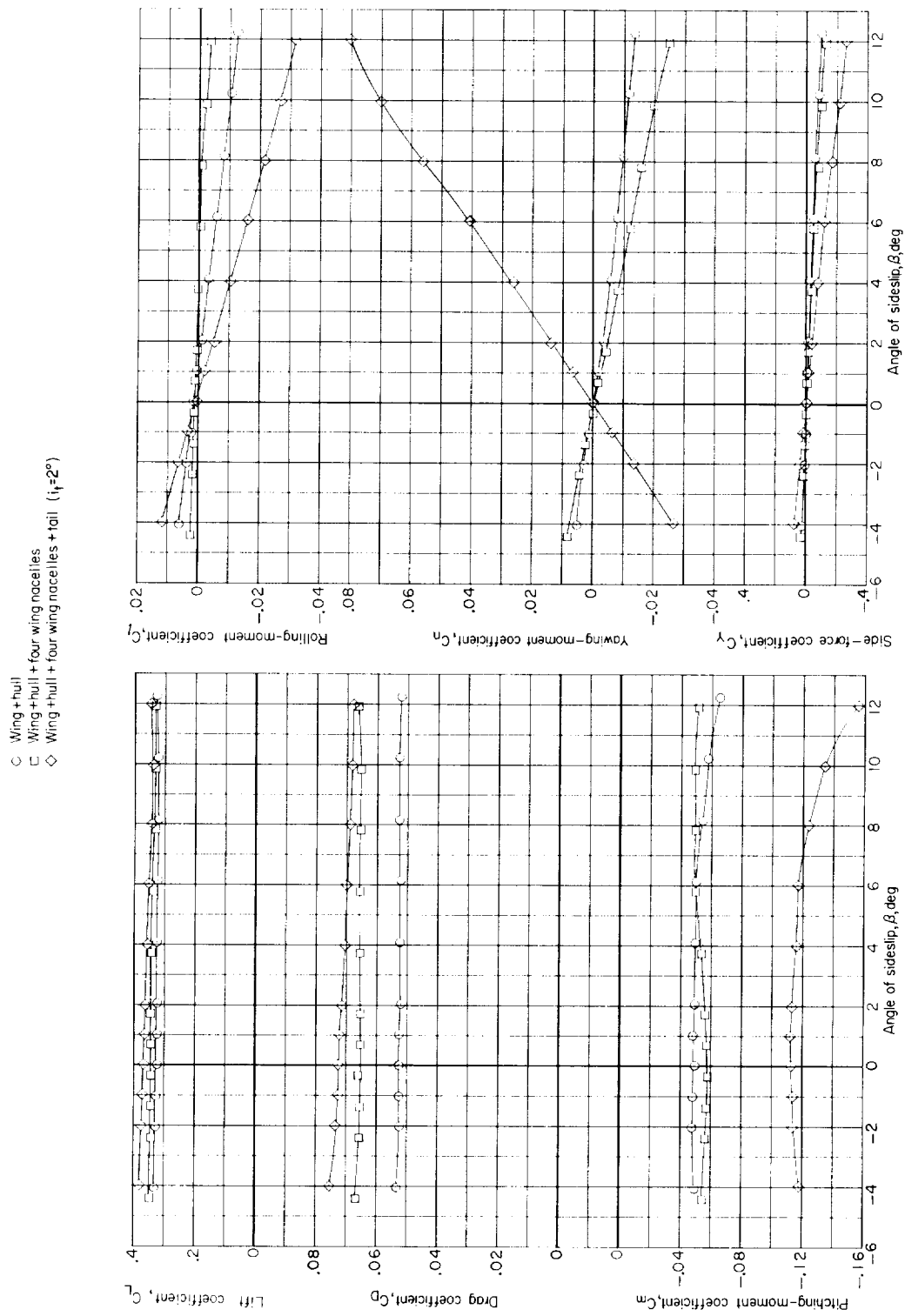
(e) $M = 1.20$.

Figure 14.- Concluded.

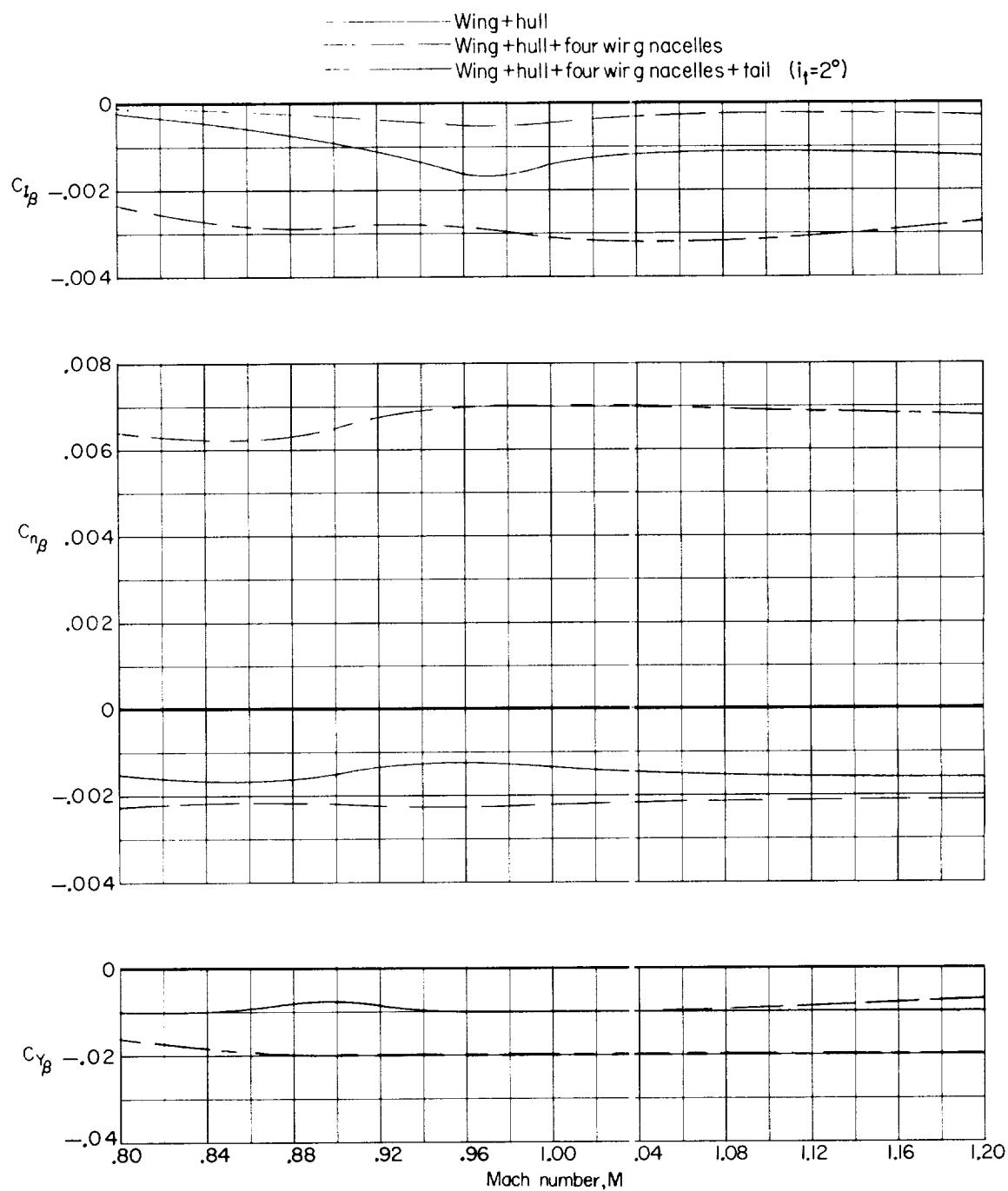


Figure 15.- Variation with Mach number of the lateral stability derivatives for the six-engine configurations. $\alpha \approx 5.7^\circ$.

<p>NASA TM X-246 National Aeronautics and Space Administration. TRANSONIC AERODYNAMIC CHARACTERISTICS OF A MODEL OF A PROPOSED SIX-ENGINE HULL- TYPE SEAPLANE DESIGNED FOR SUPERSONIC FLIGHT. Dewey E. Wormom. March 1960. 38p. OTS price, \$1.00. (NASA TECHNICAL MEMORANDUM X-246)</p> <p>The static longitudinal and lateral characteristics of a 0.02-scale model of a hull-type seaplane over a Mach number range from 0.80 to 1.20 are presented. In addition, the effects of wing leading-edge droop are included and the longitudinal aerodynamic characteristics of an alternate four-engine configuration are also presented. The wing of the configurations had an unswept 80-percent-chord line, an aspect ratio of 3.0, and a taper ratio of 0.333. The configuration also had a hull of high fineness ratio and an all-movable horizontal tail mounted on top of the vertical tail.</p> <p>NASA</p>	<p>I. Wormom, Dewey E. II. NASA TM X-246</p> <p>NASA TM X-246 National Aeronautics and Space Administration. TRANSONIC AERODYNAMIC CHARACTERISTICS OF A MODEL OF A PROPOSED SIX-ENGINE HULL- TYPE SEAPLANE DESIGNED FOR SUPERSONIC FLIGHT. Dewey E. Wormom. March 1960. 38p. OTS price, \$1.00. (NASA TECHNICAL MEMORANDUM X-246)</p> <p>The static longitudinal and lateral characteristics of a 0.02-scale model of a hull-type seaplane over a Mach number range from 0.80 to 1.20 are presented. In addition, the effects of wing leading-edge droop are included and the longitudinal aerodynamic characteristics of an alternate four-engine configuration are also presented. The wing of the configurations had an unswept 80-percent-chord line, an aspect ratio of 3.0, and a taper ratio of 0.333. The configuration also had a hull of high fineness ratio and an all-movable horizontal tail mounted on top of the vertical tail.</p> <p>NASA</p>
<p>NASA TM X-246 National Aeronautics and Space Administration. TRANSONIC AERODYNAMIC CHARACTERISTICS OF A MODEL OF A PROPOSED SIX-ENGINE HULL- TYPE SEAPLANE DESIGNED FOR SUPERSONIC FLIGHT. Dewey E. Wormom. March 1960. 38p. OTS price, \$1.00. (NASA TECHNICAL MEMORANDUM X-246)</p> <p>The static longitudinal and lateral characteristics of a 0.02-scale model of a hull-type seaplane over a Mach number range from 0.80 to 1.20 are presented. In addition, the effects of wing leading-edge droop are included and the longitudinal aerodynamic characteristics of an alternate four-engine configuration are also presented. The wing of the configurations had an unswept 80-percent-chord line, an aspect ratio of 3.0, and a taper ratio of 0.333. The configuration also had a hull of high fineness ratio and an all-movable horizontal tail mounted on top of the vertical tail.</p> <p>NASA</p>	<p>I. Wormom, Dewey E. II. NASA TM X-246</p> <p>NASA TM X-246 National Aeronautics and Space Administration. TRANSONIC AERODYNAMIC CHARACTERISTICS OF A MODEL OF A PROPOSED SIX-ENGINE HULL- TYPE SEAPLANE DESIGNED FOR SUPERSONIC FLIGHT. Dewey E. Wormom. March 1960. 38p. OTS price, \$1.00. (NASA TECHNICAL MEMORANDUM X-246)</p> <p>The static longitudinal and lateral characteristics of a 0.02-scale model of a hull-type seaplane over a Mach number range from 0.80 to 1.20 are presented. In addition, the effects of wing leading-edge droop are included and the longitudinal aerodynamic characteristics of an alternate four-engine configuration are also presented. The wing of the configurations had an unswept 80-percent-chord line, an aspect ratio of 3.0, and a taper ratio of 0.333. The configuration also had a hull of high fineness ratio and an all-movable horizontal tail mounted on top of the vertical tail.</p> <p>NASA</p>

